World Electric Vehicle Journal

MDPI

Article

Solar–Hydrogen-Storage Integrated Electric Vehicle Charging Stations with Demand-Side Management and Social Welfare Maximization

Lijia Duan, Gareth Taylor and Chun Sing Lai *

Department of Electronic and Electrical Engineering Brunel University London, London UB8 3PH, UK; lijia.duan@brunel.ac.uk (L.D.); gareth.taylor@brunel.ac.uk (G.T.)
* Correspondence: chunsing.lai@brunel.ac.uk

Abstract: The reliable operation of a power system requires a real-time balance between supply and demand. However, it is difficult to achieve this balance solely by relying on supply-side regulation. Therefore, it is necessary to cooperate with effective demand-side management, which is a key strategy within smart grid systems, encouraging end-users to actively engage and optimize their electricity usage. This paper proposes a novel bi-level optimization model for integrating solar, hydrogen, and battery storage systems with charging stations (SHS-EVCSs) to maximize social welfare. The first level employs a non-cooperative game theory model for each individual EVCS to minimize capital and operational costs. The second level uses a cooperative game framework with an internal management system to optimize energy transactions among multiple EVCSs while considering EV owners' economic interests. A Markov decision process models uncertainties in EV charging times, and Monte Carlo simulations predict charging demand. Real-time electricity pricing based on the dual theory enables demand-side management strategies like peak shaving and valley filling. Case studies demonstrate the model's effectiveness in reducing peak loads, balancing energy utilization, and enhancing overall system efficiency and sustainability through optimized renewable integration, energy storage, EV charging coordination, social welfare maximization, and cost minimization. The proposed approach offers a promising pathway toward sustainable energy infrastructure by harmonizing renewable sources, storage technologies, EV charging demands, and societal benefits.

Keywords: renewable energy; electric vehicle charging station; electric vehicle charging time uncertainty; social welfare maximization

Citation: Duan, L.; Taylor, G.; Lai, C.S. Solar–Hydrogen-Storage Integrated Electric Vehicle Charging Stations with Demand-Side Management and Social Welfare Maximization. *World Electr. Veh. J.* **2024**, *15*, 337. https://doi.org/10.3390/wevj15080337

Academic Editors: Yujie Wang and Vladimir Katic

Received: 30 June 2024
Revised: 21 July 2024
Accepted: 24 July 2024
Published: 27 July 2024

1. Introduction

The continued expansion of the world's economies has resulted in escalating energy shortages and worsening air quality. In response, low-carbon and renewable energy (RE) sources have garnered substantial interest as potential avenues to help alleviate both energy scarcity and environmental degradation. Numerous nations have enacted carbon emission regulations with the goals of curbing energy usage, boosting the efficiency of electricity production, minimizing greenhouse gas emissions, and fostering the advancement of clean energy alternatives. While conventional fossil fuel-based power generation technologies offer ample capacity and reliable operations, their overall energy utilization is inherently inefficient and inflexible in meeting fluctuations in supply and demand. Clean energy can be categorized as either renewable or non-renewable. Renewable sources encompass wind, hydroelectric, solar, geothermal, tidal, and other types. Non-renewable clean energy includes nuclear power and biomass. Renewable options provide competitively priced electricity with minimal carbon footprints; however, the intrinsic variability and intermittency of these sources inject uncertainty and volatility into energy availability.

The origins of Electric Vehicle (EV) development can be traced back to 1830 when Robert Anderson created a prototype carriage powered by electricity. However, it was not until 1884 that the first mass-produced EV was introduced by British inventor Thomas Parker [1]. Subsequently, in 1897, an electric taxi company commenced operations in New York City. Nonetheless, the EVs of that era were plagued by a multitude of issues that hindered their widespread adoption in the automotive market. A notable challenge was the inability to reliably recharge the car batteries, necessitating frequent replacement with new ones. Even in instances where recharging was possible, the limited driving range and scarcity of charging stations severely restricted the utility of EVs [2]. According to [1,2], the development of electric ignition systems for combustion engines in 1834, coupled with the availability of inexpensive fuel and gradual improvements in the reliability of gasoline-powered cars, further impeded the advancement of EVs.

Since the early 2000s, there has been a growing sense of urgency to address the greenhouse gas emissions and environmental pollution stemming from excessive reliance on fossil fuels [3]. Consequently, RE sources have increasingly become a major focal point and are now viewed as crucial alternatives in numerous countries worldwide. Notably, the electricity generation and transportation sectors are significant contributors to carbon dioxide (CO_2) emissions, accounting for approximately 64% of total emissions [3]. This situation has raised substantial public concerns regarding the potential irreversible environmental damage caused by these emissions. According to sources [4], the adoption of RE is essential for meeting carbon dioxide reduction targets in these sectors. EVs are recognized as a promising solution to control CO_2 emissions. Comprehensive research reviews [5,6] on EVs indicate that their use not only mitigates environmental impacts but also offers economic benefits to owners through lower operating costs. However, the expansion of EV charging infrastructure presents a major obstacle to increasing EV adoption [7]. Slow progress in developing charging facilities hinders potential buyers' willingness to transition to EVs [8]. Furthermore, high investment costs and uncertainties surrounding EV demand further impede infrastructure development. In London, for example, projections suggest that over 500,000 charging points will be needed by 2040, with nearly 50,000 required in public areas [9].

Figure 1 shows the Solar–Hydrogen-Storage Integrated Electric Vehicle Charging Station (SHS-EVCS), which harnesses PV, a hydrogen storage system, and battery storage to charge EVs. The station includes a solar array that converts solar power into electrical energy. This energy can be used immediately for charging EVs, fed into the grid, or stored in batteries for later use. The hydrogen storage system employs an electrolyser to split water into hydrogen and oxygen. The hydrogen is then compressed and stored for future needs. During high-demand periods, the stored hydrogen is converted back into electricity through a fuel cell to charge EVs. Additionally, a battery storage unit stores any excess energy from the solar array or the fuel cell, ensuring a steady energy supply for EV charging even when the primary renewable sources are not available.

In this paper, Section 2 provides a review of RE usage in EV charging stations (EVCSs) and the application of demand-side management (DSM) in electricity trading. Section 3 presents the problem formulation for the SHS-EVCSs. Section 4 includes a case study with forecasts for three different scenarios. Section 5 analyses the results, and Section 6 concludes by summarizing the significant findings of this paper.

The goal of this paper is to maximize social welfare, ensuring that both the SHS-EVCS and EV drivers receive the maximum possible benefits. This involves optimizing the interactions between the EVCS and EV users, aiming for a balanced and mutually beneficial outcome. By achieving this, the study seeks to demonstrate how the management of resources can lead to enhanced efficiency and satisfaction for all stakeholders involved.

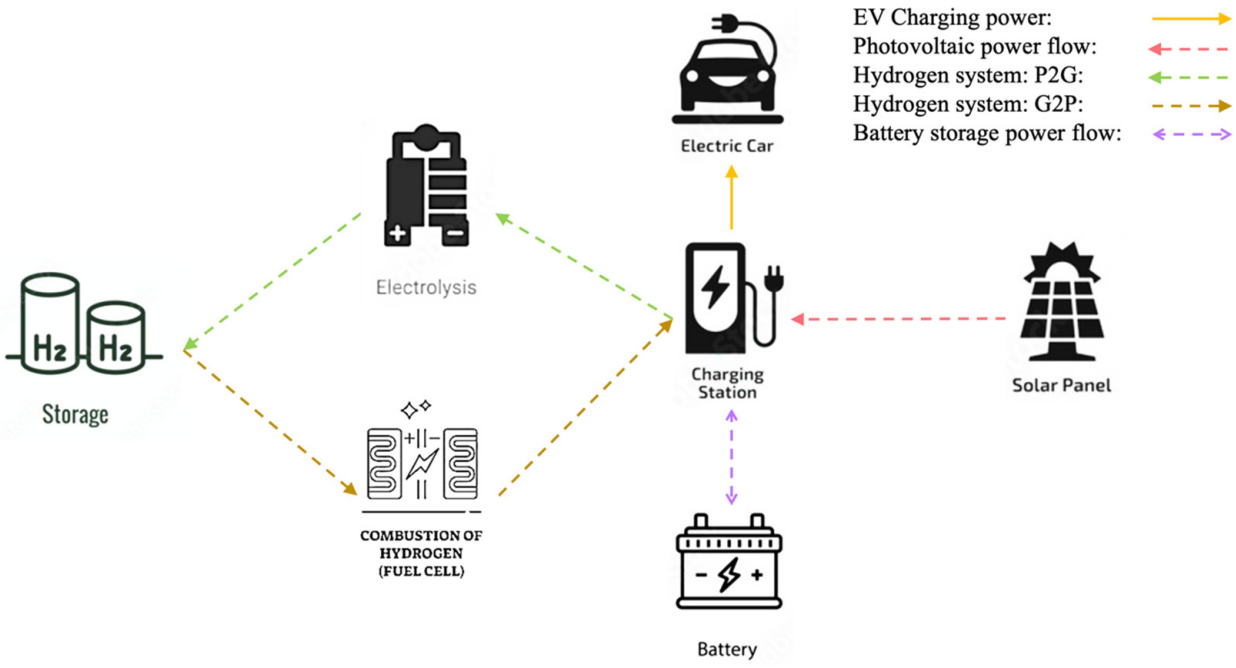

Figure 1. Single Solar–Hydrogen-Storage Integrated Electric Vehicle Charging Station topology.

2. Literature Review

To establish an efficient, resilient, and sustainable infrastructure, EVCSs can integrate RE sources [10]. Incorporating hydrogen systems, battery storage, and solar energy will play a critical role, presenting both opportunities and significant technological challenges [11]. This approach is particularly appealing for charging EVs, as battery storage systems powered by solar energy can ensure reliable charging even on cloudy days, thus improving the reliability of the charging capacity. Hydrogen tanks can store excess RE, providing high-density energy for backup power and fuel cell vehicles, thus creating versatile energy storage solutions [12]. However, integrating these diverse energy sources into a cohesive charging infrastructure poses technical challenges, with energy management being a primary concern. Ensuring efficient use, conversion, and storage of energy requires complex systems. Balancing battery solutions involves data monitoring and analysis [13]. Despite the high costs, limited lifecycle, and high-capacity features of hydrogen systems, optimizing infrastructural compatibility remains challenging, especially with the complex needs of RE installations [14]. EVCSs must accommodate large battery packs, electrolysers for clean energy production, and smart grid capabilities for dynamic energy management [14]. Interoperability issues also arise, requiring standardized interfaces and protocols to enable the seamless operation of different power generation and storage technologies. Scalability is essential to meet the increasing demand for charging stations and EVs [15]. The performance and integration of RE systems can be enhanced through advanced EV charging stations. Machine learning and artificial intelligence can improve energy management systems, optimizing the integration of supply and demand [16]. Innovations in battery technology, including solid-state batteries, will enable fast charging times and high energy densities, potentially transforming battery storage options at EV charging stations [17,18]. Additionally, hydrogen production efficiency driven by RE through green electrolysis can reduce costs, enhancing scalable energy storage solutions in EV charging infrastructure [19]. Paper [20] proposes a strategy to optimize small-scale PV systems for homes, reducing energy costs by up to 40% and allowing for extra loads without expanding the network, while addressing EV charging and unsynchronized demand challenges. A review [21] examined advancements in energy storage from 1850 to 2022, highlighting their evolution, principles, and role in addressing renewable energy intermittencies to help decarbonize the environment.

Demand-Side Management (DSM) is a key strategy within smart grid systems, encouraging end-users to actively engage and optimize their electricity usage [22,23]. DSM implements various measures to help consumers plan and use electricity more rationally and efficiently, thereby improving the efficiency of terminal electricity consumption. Additionally, DSM is crucial in resource allocation by adapting to demand-side participation in power market management, which helps prevent large-scale power outages due to peak loads or the need for additional power generation infrastructure, ultimately reducing costs within the smart grid system [24]. In power market transactions, electricity's unique characteristics—being instantly consumable and hard to store—require rapid data exchange, swift decision-making, and real-time adjustments from both supply and demand sides. This level of responsiveness is difficult to achieve in traditional power grids. However, in smart grid systems, advanced technologies like smart meters, smart homes, and cloud computing significantly enhance DSM capabilities [25,26].

As the energy Internet evolves, it enables the integration of multiple energy sources and dynamic management practices. This transformation allows for more sustainable and efficient energy consumption patterns, aligning with the shift towards comprehensive, interconnected energy networks. Demand response (DR) is a vital mechanism where electricity consumers adjust their power usage in response to market signals or incentives from power suppliers [27]. DR is a critical component of DSM, and studies have shown that it significantly improves end-use electricity consumption efficiency, reduces resource waste due to supply–demand imbalances, and contributes to overall grid stability [28,29]. The rapid development of smart grids, incorporating technologies like smart homes and EVs, provides substantial support for DR initiatives. Furthermore, DR benefits consumers by reducing electricity bills through altering traditional consumption patterns and strategically shifting usage away from peak periods, helping to prevent large-scale power outages [30]. As distributed energy resource integration progresses, the synergy between regional energy systems—including various forms of energy generation and storage—and power grid systems has transitioned DR from a conventional approach to a holistic strategy of managing diverse load types, such as wind, solar, electrical, and storage. This evolution has normalized DR integration into power system dispatch strategies, highlighting its growing importance in achieving a more resilient and efficient energy landscape [31,32]. Integrating DR into energy management enhances operational flexibility and optimizes the economic operation of power systems by maximizing resource utilization. The increasing presence of RE sources and their variability in the power grid further emphasize the need for sophisticated DR strategies.

Maintaining stable power system operations necessitates a real-time balance between supply and demand. However, achieving this balance solely through supply-side regulation is challenging. Therefore, effective DSM measures are crucial [33]. Real-time pricing, as the most direct and effective DSM method, employs electricity price signals to encourage consumers to voluntarily shift their electricity usage to off-peak periods, thereby reducing peak loads and achieving the objectives of peak shaving and valley filling [33,34]. Study [35] pioneered the application of the social welfare maximization model to real-time pricing in smart grids. The goal was to maximize user utility while minimizing the power provider's costs, with the objective function being the user's utility minus the provider's cost. This study established a social welfare maximization model for smart grid real-time pricing, subject to the constraint of power supply and demand balance. It utilized a dual optimization method to determine supply, electricity consumption, and real-time electricity prices [35].

Societal welfare has long been a fundamental preoccupation, and the interplay between individual needs and collective interests forms the crux of modern social welfare discourse. "Social welfare" emerges as the outcome of public choices regarding the distribution of societal benefits within specific institutional frameworks, representing a collective or group interest [36]. On the other hand, "utility" denotes the psychological satisfaction derived by consumers during the consumption process. Economics employs these two fundamental

notions of welfare and utility to elucidate and illustrate the potential balance between personal motivations and social choices [34]. Table 1 shows the relevant work.

Table 1. Literature review and benchmarking of relevant work.

Reference	Electricity Sources	P2P and Game Theory Applied	EV/RE Uncertainty Prediction	Include Social Welfare	Multi-EVCSs Energy Exchange
[37]	Wind, PV, battery energy storage, grid	No	Yes	No	No
[38]	Wind, PV, battery energy storage, grid	Yes	Yes	Yes	No
[39]	Grid	Yes	Yes	No	No
[40]	PV, wind	No	Yes	Yes	No
[41]	Energy management system	No	Yes	No	No
[42]	Battery storage system	No	Yes	No	No
[43]	Wind, PV, battery energy storage, grid	No	No	No	No
[44]	Grid, PV, wind	No	Yes	No	No
[45]	PV, battery energy storage, hydrogen storage, grid	No	No	No	Yes
[46]	PV, battery energy storage, hydrogen storage, grid	Yes	No	No	Yes
This work	PV, battery energy storage, hydrogen storage, grid	Yes	Yes	Yes	Yes

This paper examines the practical feasibility of EVCSs through two primary models. The first is a non-cooperative game model for a single charging station aimed at minimizing construction, operation, and maintenance costs. The second model is the internal EVCS energy transaction cooperation model, expanded from [46], which integrates operational load and an internal dispatch center for demand response. Additionally, a model focuses on maximizing social welfare by considering the economic interests of EV owners, including acceptable charging prices, essentially minimizing the cost of electricity supply. In the general social welfare model, another significant factor is the capital cost of the electricity provider (grid, RE, storage systems, etc.). However, in the SHS-EVCS model, this capital cost is calculated in the non-cooperative game model for a single charging station and is, therefore, excluded from the social welfare maximization model.

This paper makes three main contributions:

- Develops an EV charging time model using a Markov decision process to address uncertainties in charging times and a Monte Carlo simulation to assess and predict EV charging demand, which is expected to fluctuate based on probabilities associated with different charging times.
- Creates a bi-level optimization model that combines non-cooperative and cooperative game theory to minimize capital costs and maximize social welfare.
- Improves the social welfare maximization real-time pricing model based on the dual theory, considering the benefits to drivers, the SHS-EVCS, and the grid side, according to EV charging demand.

3. Problem Formulation

This paper organizes the multi-SHS-EVCS system into two distinct levels. The first level focuses on an individual SHS-EVCS, employing a non-cooperative game theory model to reschedule energy dispatch with the aim of minimizing capital costs. The second level, similar to the approach in paper [46], but introduces an Internal Management System (IMS),

also known as a demand response centre, into the SHS-EVCS coalition to manage the sequencing of charging and discharging activities. At this level, the goal is to maximize the coalition's profit. The ultimate objective of this bi-level model is to maximize social welfare.

3.1. First-Level SHS Model

This section combines solar energy, hydrogen storage, battery storage (SHS), and the grid into a non-cooperative game theory model for EVCS. In this model, hydrogen storage provides long-term energy buffering, batteries offer quick responses to demand changes, solar energy adds renewable generation, and the grid ensures a stable supply. The goal is to minimize construction, operation, and maintenance costs while optimizing energy distribution. Figure 2 illustrates the specific interaction model.

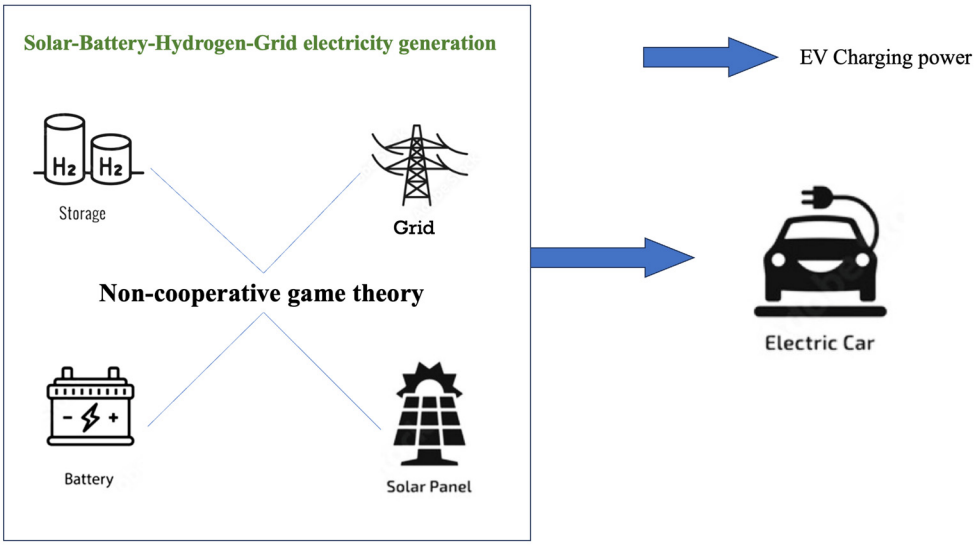

Figure 2. Electricity dispatch depends on non-cooperative game theory within SHS system.

The problem formulation of the first level's objective function is given in reference [45] in Equations (1) and (3)–(10).

3.1.1. Non-Cooperative Game Theory

The model discussed in this section is a multi-agent framework where each piece of equipment aims to minimize costs independently. The strategic decisions of each participant are made without considering others, creating a scenario of mutual interaction and fair competition, typical of a non-cooperative game model. The interactions among all energy sources can be described as follows:

$$G = \{P; N; E\} \tag{1}$$

where P represents the game players, N is the strategy set, and E is the payoff function.

- Game player: In this context, each decision-making entity is referred to as a game player. The participants in this study include solar energy (S), hydrogen energy storage (H), battery energy storage (B), and the power grid (G). These participants are collectively represented as

$$P = \{S,\ H,\ B,\ G\} \tag{2}$$

- Strategy Set: Each participant selects a set of strategies during the game to maximize their benefits, which in this context means minimizing costs. The strategies for each energy source are solar energy (N_S), hydrogen energy storage (N_H), battery energy storage (N_B), and the power grid (N_G). The strategy set is

$$N = \{N_S;\ N_H;\ N_B;\ N_G\} \tag{3}$$

- Payoff: The payoff function assesses each participant's cost and provides feedback for strategy adjustments in subsequent rounds. The payoff for each participant depends on their strategy and the strategies of others, represented as

$$E_{SHS}(N_S;\ N_H;\ N_B;\ N_G) \tag{4}$$

where E_{SHS} is the minimum cost for the SHS system.

Non-cooperative games aim to find a Nash equilibrium, achieving the optimal objective function. To meet the Nash equilibrium condition, minimizing the grid's cost means reducing power purchases from the grid. Therefore, the optimal solution for the grid P_g^t requires fixing the power outputs of P_{pv}^t, P_{hs}^t, and P_{es}^t. Similarly, for the optimal solutions of solar power P_{pv}^t, battery storage P_{es}^t, and hydrogen storage P_{hs}^t, the power outputs of the other sources must be fixed.

Step to solve Nash Equilibrium:

(1) Initialization: set initial strategies N_S, N_H, N_B, N_G; replace by P_g^t, P_{pv}^t, P_{hs}^t, and P_{es}^t.

(2) Iterative optimization:
   - Grid:
     - Fix P_{pv}^t, P_{hs}^t, and P_{es}^t.
     - Solve the optimal P_g^t.
   - Solar power:
     - Fix P_g^t, P_{hs}^t, and P_{es}^t.
     - Solve the optimal P_{pv}^t.
   - Battery storage:
     - Fix P_g^t, P_{hs}^t, and P_{pv}^t.
     - Solve the optimal P_{es}^t.
   - Hydrogen storage system:
     - Fix P_g^t, P_{es}^t, and P_{pv}^t
     - Solve the optimal P_{hs}^t.

(3) Check convergence:
   - Verify if all participants' strategies converge to a fixed point. If not, return to Step 2 for further iteration.

4. Verify Nash Equilibrium:
   - Ensure all strategy combinations meet the Nash equilibrium condition, where no participant can further reduce its cost by changing its strategy while others' strategies remain unchanged.

3.1.2. EV Uncertainty Model

To capture the variability in EV charging times, this paper uses a Markov chain probability model. This model is ideal for describing random processes with discrete time intervals and states, where the future state depends solely on the current state, not on the sequence of previous states. The use of transition probabilities between adjacent states simplifies the complexity of the random process. Each battery power level of an EV can be considered a discrete state, with the random fluctuations in battery power represented as a non-stationary Markov chain. This chain effectively models the likelihood of an event occurring based solely on the present state [47].

$$P\left\{x_f^{dis}\middle|x_1^{dis}=s_1^{dis},\ x_2^{dis}=s_2^{dis},\ldots,x_{f-1}^{dis}=s_{f-1}^{dis}\right\}=P\left\{x_f^{dis}\middle|x_{f-1}^{dis}=s_{f-1}^{dis}\right\} \tag{5}$$

$$s_f^{dis} \in S^{dis},\ 1 \le f \le f_{max}$$

where x_f^{dis} is the $f'th$ discrete variable; s_f^{dis} is the $f'th$ discrete state; S^{dis} is the discrete state space; f_{max} is the maximum number of discrete variables.

Based on (5), it is also needs to satisfy

$$P\left\{x_f^{dis}\middle|x_{f-1}^{dis}=s_{f-1}^{dis}\right\}=P\left\{x_{f+1}^{dis}\middle|x_f^{dis}=s_f^{dis}\right\} \tag{6}$$

To capture the randomness and reversibility of EV charging and driving power consumption, the Markov sampling process incorporates the detailed balance condition. This condition ensures that transitions between any two states are reversible:

$$p_{ij}P\left\{x_{f+1}^{dis}=s_j^{dis}\middle|x_f^{dis}=s_i^{dis}\right\}=p_{ji}P\left\{x_{f+1}^{dis}=s_i^{dis}\middle|x_f^{dis}=s_j^{dis}\right\} \tag{7}$$

where p_{ij} is the transition probability of state i to j; p_{ji} is the transition probability of state j to i.

EVs can be classified into two operational states: charging and non-charging. These correspond to two modes: charging mode and waiting mode [47–50]. In the charging mode, the EV is connected to the SHS-EVCS and is actively charging. Conversely, in the waiting mode, the EV is at the SHS-EVCS but not charging, meaning it is in a parked state. The variable c_f represents the charging probability, capturing the randomness of EV charging, while d_f denotes the probability of interrupted charging, reflecting the variability within the charging process.

The state transition probabilities are illustrated in Figure 3. In this context, EVC_f and EVD_f represent the states of the charging mode and waiting mode, respectively. The transition probabilities between these states are denoted by d_f and c_f, while a_f signifies the waiting probability. ΔT_1 and ΔT_2 correspond to the charging time and waiting time, respectively. All the arrows represent the probability to change the charging or discharging state.

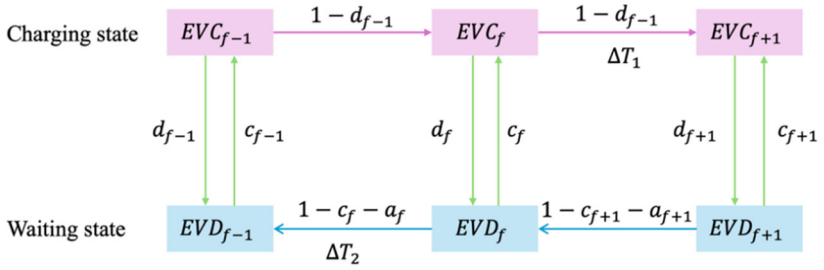

Figure 3. State transition diagram.

If the EV drivers are anxious of battery level, in this paper, the level is $B_{min}^{arrive} \le 35\%$, which means if the EV battery's SOC is less than or equal to 35%, the drivers will charge their EV. When charging the car, if $B_{min}^{leave} \ge 95\%$, the EV drivers will choose to discharge their cars. N is the full battery level which is 100. The probability for c_f and d_f can be demonstrated as [47–49]:

$$c_f=\begin{cases}\frac{1}{1+e^{\left(f-0.5\left(B_{min}^{arrive}+N\right)\right)^{0.14}}} & f \ge B_{min}^{arrive}\\ 0 & f < B_{min}^{arrive}\end{cases} \tag{8}$$

$$d_f=\begin{cases}\frac{1}{1+e^{\left(0.5\left(B_{min}^{leave}+N\right)-f\right)^{0.32}}} & f \ge B_{min}^{leave}\\ 1 & f < B_{min}^{leave}\end{cases} \tag{9}$$

The state probability EVC_f and EVD_f of EV can be denoted as [45–47]

$$P_s\left(EVC_f\right) = \begin{cases} \left(1-d_{f-1}\right)P_s\left(EVC_{f-1}\right) + c_f P_s\left(EVD_f\right) \\ 1 \le f \le N \\ c_0 P_s(EVD_0) \\ f = 0 \end{cases} \tag{10}$$

$$P_s\left(EVD_f\right) = \begin{cases} d_f P_s\left(EVC_f\right) + a_f P_s\left(EVD_f\right) + \left(1-c_{f+1}-a_{f+1}\right)P_s\left(EVD_{f+1}\right) \\ 0 \le f \le N-1 \\ d_N P_s(EVC_N) + a_N P_s(EVD_N) \\ f = N \end{cases} \tag{11}$$

where $Ps(EVC_f)$ is the state probability of EVC_f, and $Ps(EVD_f)$ is the state probability of EVD_f.

These variables are subject to

$$\sum_{f=0}^{100}\left\{P_s\left(EVC_f\right) + P_s\left(EVD_f\right)\right\} = 1 \tag{12}$$

$$\mathrm{d}_0 = 0,\ \mathrm{c}_0 = 1,\ \mathrm{d}_{100} = 1,\ \mathrm{c}_{100} = 0 \tag{13}$$

where (12) indicates that the total sum of all state probabilities of the EV at any given time is equal to 1; (13) denotes that when the battery level is equal to 0, it must be in the EVC_f mode, and when the battery is in a full state, it must be in the EVD_f mode.

ΔT_1 and ΔT_2 are [47]

$$\Delta T_1 = min\left\{\frac{B_{cap}\Delta(+f)}{N\eta_c P_c},\ T_{leave} - T_{arrive}\right. \tag{14}$$

$$\begin{cases} \Delta T_2 = \frac{B_{cap}\Delta(-f)}{NE_{km}v} \\ 1 \le \Delta(-f) \le N \end{cases} \tag{15}$$

where

- η_c is the EV battery efficiency, which is 95;
- P_c is the fixed charging power, which is 7 kW;
- B_{cap} is the battery capacity, which is 60 kWh (Tesla model 6 battery capacity);
- $\Delta(-f)$ is the electricity loss when driving the EV;
- E_{km} is energy consumption, which is 16.25 kWh/100 km;
- v is the average driving speed, which is 32 km/h.

To predict the electricity demand for all SHS-EVCSs catering to numerous EV drivers, it is crucial to first establish a prediction model for the charging demand of a single EV. Following this, the overall electricity demand of EVs can be calculated by aggregating the individual EV charging demands using the Monte Carlo random simulation method. The total charging power demand at any specific time can be represented as follows:

$$P_{cha,sum} = \sum_{i}^{N_{ev}} P_{cha,i} \tag{16}$$

where $P_{cha,sum}$ is the total charging power; $P_{cha,i}$ is the i'th EV charging power; N_{ev} is the total EV number.

For each EV's SOC, it should follow

$$SOC_{start} = \frac{1}{SOC_{start,max} - SOC_{start,min}} \tag{17}$$

where SoC_{start} is the initial SoC of the EV; $SoC_{start,max}$ and $SoC_{start,min}$ are the maximum and minimum SoC of the EV.

For the EV's battery SoC_{arrive} when arriving at SHS-EVCS, it is denoted as

$$SOC_{arrive} = SOC_{start} - \frac{D_{EV} E_{km}}{B_{cap}} \tag{18}$$

where D_{EV} is the EV's driving distance and subject to

$$0 \leq D_{EV} < \frac{B_{cap}}{E_{km}} \tag{19}$$

Meanwhile, for all the EV drivers, they have z times charging opportunities [51]:

$$1 \leq z \leq 3 \tag{20}$$

While the Monte Carlo method is known for its high prediction accuracy, it requires an understanding of the probability distribution of the input samples. Predicting EV charging demand involves many uncertain factors that often do not adhere to a standard probability distribution, making it challenging to determine the corresponding probability density function [47]. For example, the probability of EV owners choosing a simple travel chain for commuting and the likelihood of EVs charging from the grid usually fall under discrete probability distributions [47–49]. Hence, it is necessary to first establish the probability distribution of the uncertain factors before applying the Monte Carlo method to predict EV charging demand. The algorithm for forecasting EV charging is as follows (Algorithm 1):

Algorithm 1: EV Charging Demand Forecast Algorithm

Input: the EV data: B_{cap}, η_c, P_c, E_{km}, v, N_{ev}...

(a) Repeat 1: calculate the EV's charging demand
(b) Get initial EV data SoC_{start}, $P_{cha,sum}$ through Monte Carlo random simulation method
(c) Repeat 2: calculate single EV charging demand
(d) Update the current battery level
(e) Calculate the charging and discharging probability c_f, d_f
(f) Calculate the charging duration ΔT_1
(g) Calculate the waiting duration ΔT_2
(h) Obtain the charging frequency $1 \leq z \leq 3$
(i) Repeat 2 to calculate the single EV charging demand
(j) End repeat 2
(k) Repeat 1 based on (17) to obtain the total EV charging demand
(l) End repeat 1

End: Output the total EV charging demand to obtain the SHS-EVCS charging load

3.2. Second-Level Social Welfare Model

The second level adopts a similar approach to [46], utilizing a game theory-based P2P energy exchange process, while integrating aspects of information transfer and load demand considerations. Figure 4 illustrates the operation of this level: the blue line depicts internal P2P energy trading, demonstrating the exchange of energy among the SHS-EVCSs. The pink line indicates the flow of information, outlining the communication pathways between each EVCSs and the central information hub, as well as between the EVCSs and individual EVs. The yellow line symbolizes the flow of EV charging information, with each EVCS gathering data when EVs are either charging or waiting to charge. These data feed into the Markov decision process to accurately forecast EV charging demand in a real-time scenario.

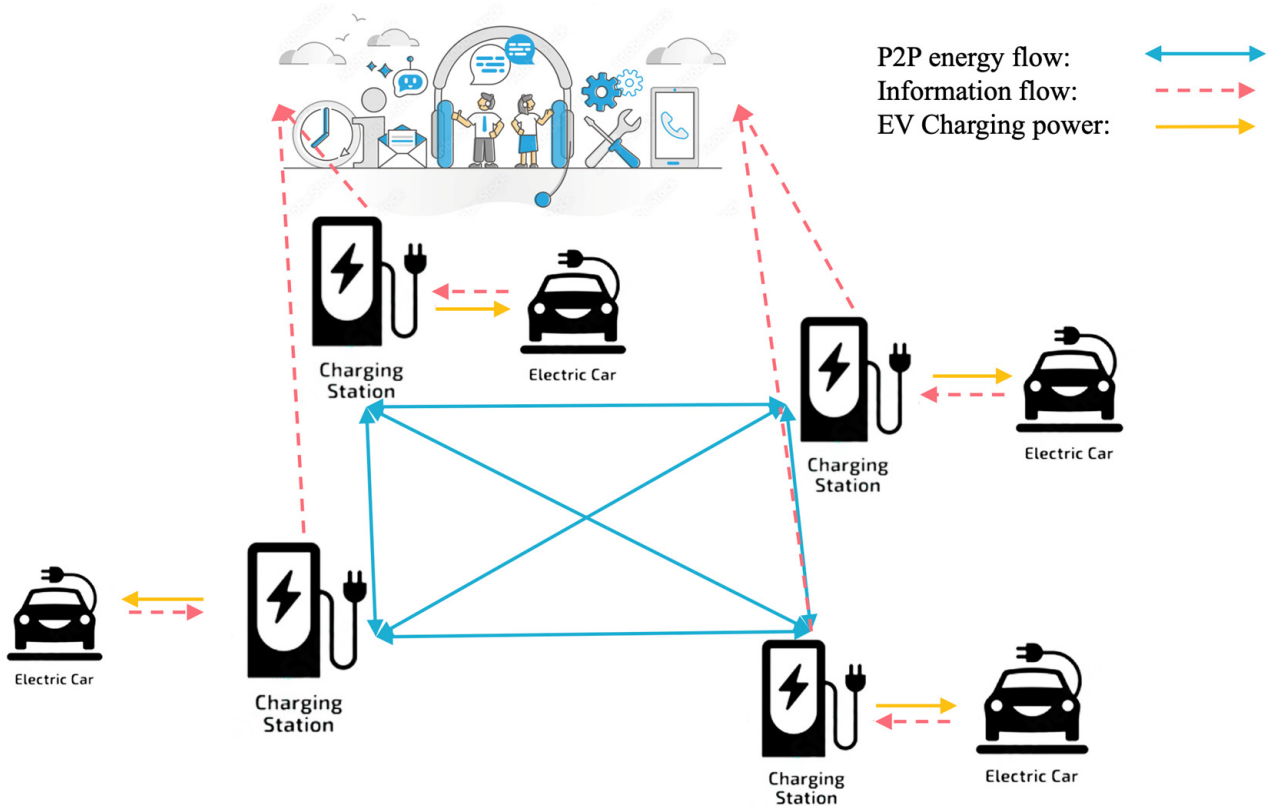

Figure 4. Topology for SHS-EVCSs coalition information and energy flow.

Within the SHS-EVCSs coalition, which includes four EVCSs, D users, and an IMS, each SHS-EVCS produces electricity to satisfy the demand of EV drivers within its locale. They are interconnected through a communication network that facilitates the exchange of real-time data on electricity prices and power requirements. The power consumption cycle is segmented into k time periods. At the start of each period, the IMS determines an electricity price reflecting the current power market conditions. Both EV drivers and SHS-EVCSs gauge their optimal power usage and generation based on this pricing and communicate their data back to the IMS. The IMS then adjusts the electricity price in response to the incoming data on consumption and supply. This cyclical adjustment process persists, with both drivers and SHS-EVCSs tuning their power usage and output to align with the updated pricing information. This exchange continues until equilibrium is reached between supply and demand, thus setting the electricity price for that interval. The established price then serves as the real-time electricity rate for that time.

The problem formulation of the game theory and P2P process is giving in paper [46]; this level considers social welfare maximization, and the formulation is as follows. A novel price-based real-time electricity pricing model [35,52,53] is introduced to optimize the gap between the total utility of the EV driver and the costs incurred by the electricity provider (SHS-EVCS). This sets up the subsequent optimization challenge:

$$max \sum_{k=1}^{K} \left(\sum_{d=1}^{D} V_1\left(x_d^k,\ \omega_d^k\right) - C_k(G_k) \right) \tag{21}$$

$$s.t.\ \sum_{d \in D} x_d^k \le G_k,\ k = 1, 2, \ldots, K,$$

$$x_d^k \ge 0,\ k = 1, 2, \ldots, K.$$

The social welfare maximization model (21) can be defined as:

$$max \sum_{k=1}^{K} \left(\sum_{d=1}^{D} V_d\left(x_d^k,\ \omega_d^k\right) - C_k(G_k) \right) \tag{22}$$

$$s.t.\ \sum_{d\in D} x_d^k \le G_k,\ k = 1, 2, \ldots, K$$
$$m_d^k \le x_d^k \le M_d^k,\ d = 1, 2, \ldots, D; k = 1, 2, \ldots, K$$
$$G_k^{min} \le G_k \le G_k^{max},\ k = 1, 2, \ldots, K$$

where x_d^k is the electricity consumption of EV driver d at time k; m_d^k and M_d^k are the minimum and maximum electricity consumptions of EV driver d at time k, and they satisfy $m_d^k \le x_d^k \le M_d^k$; G_k is SHS-EVCS's electricity supply at time k; G_k^{min} and G_k^{max} are the minimum and maximum electricity supplies of the SHS-EVCS, and $G_k^{min} \le G_k \le G_k^{max}$; generally, $G_k^{min} \ge \sum_{d=1}^{D} m_d^k$ and $G_k^{max} \ge \sum_{d=1}^{D} M_d^k$; $C_k(G_k)$ means the cost for the SHS-EVCS to provide electricity for G_k at time k, and it is the convex function of G_k; C_k is the capital cost for SHS-EVCS from first-level output; $V_d\left(x_d^k,\ \omega_d^k\right)$ is the utility of EV driver d using x_d^k at time k, and it is the concave function of x_d^k; ω_d^k is driver d's elasticity of charging his EV at time k, for $\omega_d^k \in [1,\ 3.5]$.

The objective function aimed at maximizing social welfare is concave, and the associated constraints form a convex set. Consequently, this constitutes a convex programming issue that can be efficiently resolved using standard convex programming methods. In Equation (22), the critical decision variables are the electricity consumption of the driver, x_d^k, and the power supply from SHS-EVCS, G_k. However, the real-time electricity price, a central variable in the model, is absent, rendering a direct solution to Equation (22) unfeasible. In convex optimization, the original problem can often be mirrored by a dual problem where the dual decision variables, namely, the Lagrange multipliers from the Lagrange function of the original problem, equate to the shadow prices in economic theory. These shadow prices are deemed theoretically optimal for pricing. Consequently, this work applies the dual theory to effectively determine the real-time electricity pricing [34,35,54–56].

Each interval in (22) is independent of each other, so a distributed algorithm can be used to solve each interval separately. The optimization problem corresponding to the k-th interval is

$$max \sum_{d=1}^{D} V_d\left(x_d^k,\ \omega_d^k\right) - C_k(G_k) \tag{23}$$
$$s.t.\ \sum_{d=1}^{D} x_d^k \le G_k$$
$$m_d^k \le x_d^k \le M_d^k,\ d = 1, 2, \ldots, D$$
$$G_k^{min} \le G_k \le G_k^{max}$$

The Lagrange function for (23) is denoted as

$$L\left(x_d^k,\ G_k, \lambda_k\right) = \sum_{d=1}^{D} V_d\left(x_d^k,\ \omega_d^k\right) - C_k(G_k) + \lambda_k(G_k - \sum_{d=1}^{D} x_d^k) \tag{24}$$
$$= \sum_{d=1}^{D}(V_d\left(x_d^k,\ \omega_d^k\right) - \lambda_k x_d^k) + (\lambda_k G_k - C_k(G_k)) \tag{25}$$

where $\lambda_k > 0$ is the Lagrangian multiplier, and according to the dual theory, (23) can be transform to

$$\min \max\ L\left(x_d^k,\ G_k, \lambda_k\right) \tag{26}$$

where $\lambda_k > 0$, $x_d^k \in \left[m_d^k, M_d^k\right]$, $G_k \in \left[G_k^{min},\ G_k^{max}\right]$.

Remark:

$$x_d^{k*} = argmax\left((V_d\left(x_d^k,\ \omega_d^k\right) - \lambda_k x_d^k\right) \tag{27}$$
$$x_d^k \in \left[m_d^k, M_d^k\right]$$
$$G_k^* = argmax(\lambda_k G_k - C_k(G_k)) \tag{28}$$
$$G_k \in \left[G_k^{min},\ G_k^{max}\right]$$

$$A(\lambda_k) = \max\ L\left(x_d^k,\ G_k, \lambda_k\right) \tag{29}$$

$$x_d^k \in \left[m_d^k, M_d^k\right]$$

$$G_k \in \left[G_k^{min},\ G_k^{max}\right]$$

$$= \sum_{d=1}^{D}(V_d\left(x_d^{k*},\ \omega_d^k\right) - \lambda_k x_d^{k*}) + (\lambda_k G_k^* - C_k(G_k^*)) \tag{30}$$

If λ_k represents the Time of Use (TOU) or real-time electricity price for the k-th interval, then Equation (27) defines the driver's optimal electricity consumption for charging that maximizes personal welfare (by balancing utility gain against the cost of electricity). Equation (28) shows how the SHS-EVCS optimizes its welfare by maximizing the difference between revenue from electricity sales and the cost of power supply to determine the optimal electricity provision for charging. Therefore, it is logical to use the Lagrangian multiplier λ_k as the real-time electricity price.

To address the dual problem, where the goal is to minimize $A(\lambda_k)$, with $\lambda_k > 0$, the following method can be employed [57,58]:

$$\lambda_k^{h+1} = \lambda_k^h + \gamma_k^h a_k^h \tag{31}$$

where h is the iteration time; γ_k^h is the distance and ≥ 0; a_k^h is the downward direction of function $A(\lambda_k)$; let $a_k^h = \sum_{d=1}^{D} x_d^{k*} - G_k^*$; (31) proves that when $\sum_{d=1}^{D} x_d^{k*} > G_k^*$, $a_k^h > 0$, while $\lambda_k^{h+1} > \lambda_k^h$ due to the demand and supply theory, and the electricity price increases; when $\sum_{d=1}^{D} x_d^{k*} < G_k^*$, $a_k^h < 0$, then $\lambda_k^{h+1} < \lambda_k^h$, and the electricity price decreases; when $\sum_{d=1}^{D} x_d^{k*} = G_k^*$, while $\lambda_k^{h+1} = \lambda_k^h$, the electricity price stays balanced. In paper [30,34,51], γ is a fixed positive number, which is 0.8. Figure 5 shows the power and information interaction between SHS-EVCS, EV drivers, and IMS. Real-time electricity price distributed algorithm shows in Algorithm 2.

Algorithm 2: Real-time electricity price distributed algorithm

Initialization parameters: γ, D, k, m_d^k, M_d^k, and stop error ε (ε is a positive number 0.1), for h = 0. The IMS randomly releases electricity price λ_k^h to the SHS-EVCS and EV driver.

1. According to the random electricity price, use (26) to calculate the optimal electricity consumption $x_d^{k*}\left(\lambda_k^h\right)$ by the EV driver and report the optimal electricity consumption to the ISM.
2. Use $G_k^* = argmax(\lambda_k G_k - C_k(G_k))$ to calculate the optimal electricity supply $G_k^*\left(\lambda_k^h\right)$ by the SHS-EVCS, and report it to the ISM.
3. Accept the optimal $x_d^{k*}\left(\lambda_k^h\right)$ and $G_k^*\left(\lambda_k^h\right)$, using $\lambda_k^{h+1} = \lambda_k^h + \gamma_k^h a_k^h$ to calculate the optimal electricity price.
4. If $0 < G_k^*\left(\lambda_k^h\right) - \sum_{d=1}^{D} x_d^{k*}(\lambda_k^h) \leq \varepsilon$, let $\lambda_k = \frac{1}{2}\left(\lambda_k^h + \lambda_k^{h+1}\right)$; if not, input λ_k^{h+1} to 1

End: output the optimal solution for x_d^{k*} and G_k^*

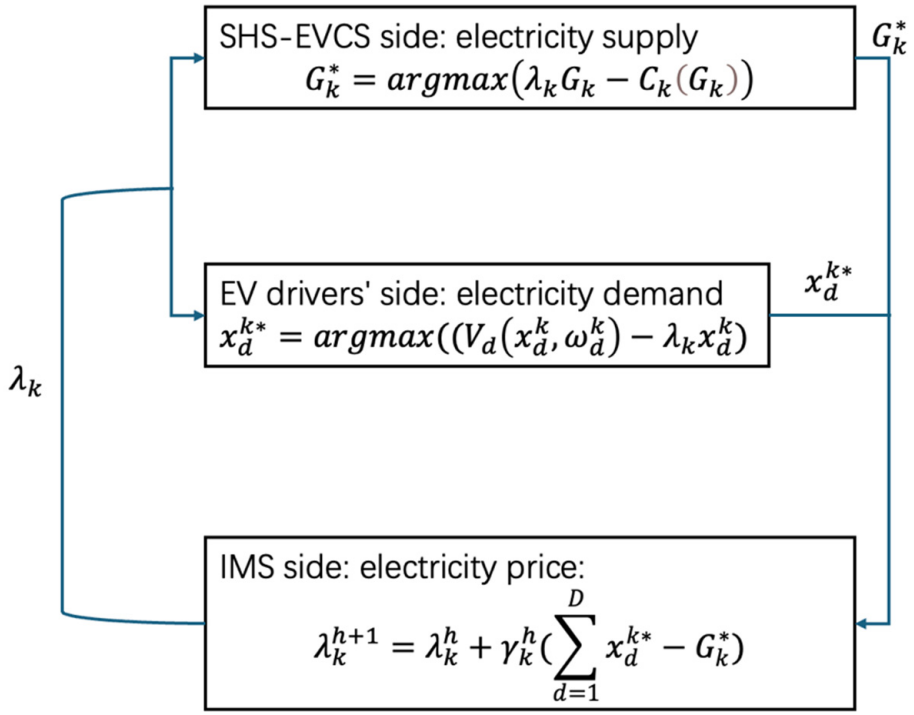

Figure 5. Power and information interaction between SHS-EVCS, EV drivers, and IMS.

4. Case Study

Three scenarios are explored in this analysis: the first involves day-ahead forecasting without the Time-of-Use (TOU) strategy, focusing on uncertainties associated with EVs. The second scenario extends this to include real-time forecasting alongside day-ahead predictions without a TOU strategy. The third introduces both day-ahead and real-time forecasts with an active TOU strategy.

In the TOU scenarios, load management decisions are proactively shaped by anticipated demand and supply data from the transportation department, enabling planning and optimization of energy resources. In contrast, the real-time TOU scenario leverages a Markov decision process to dynamically adjust and optimize the load based on actual data. This approach compares fixed loads, which are immutable and must be met under any circumstances, with flexible loads that can be adjusted based on real-time information. The objective is to assess the impact of these load adjustments on social welfare, with the goal of enhancing efficiency, reducing costs, and improving the synchronization of energy supply and demand.

Table 2 and Figure 6 show the initial scenario that involves fixed loads, where SHS-EVCS parameters are based on the forecasting and scheduling methods based on transport statistics from gov.uk, which is addressed in paper [59]. In Figure 6, the fixed load values for Hammersmith & Fulham and Hounslow are based on weekday averages, which is why the charging peaks occur before and after working hours. The fixed load values for the other two EVCSs are based on weekend averages. Figure 7 displays the SHS-EVCS's load curves for day-ahead and real-time forecasts under a non-TOU framework, showing that variables such as EV charging times, arrival and departure battery capacities, and charging rates remain constant.

Table 2. Four London areas' SHS-EVCS parameters [45,46,60,61].

Parameters	Hammersmith & Fulham	Richmond upon Thames	Hounslow	Ealing
Charger capacity (kW)	360	360	360	360
Number of chargers per station	3	8	14	21
PV installed capacity (kWp)	500	1000	1000	1000
PV installation cost (£/kWp)	1112	1112	1112	1112
Battery capacity (kWh)	1000	800	800	800
Battery installed cost (£/kWh)	331.55	331.55	331.55	331.55
Battery initial state of charge (%)	40	40	40	40
Rated charge and discharge power of battery (kWh)	500	500	500	500
Minimum battery state of charge (%)	25	25	25	25
Maximum battery state of charge (%)	100	100	100	100
Battery charge and discharge efficiency (%)	85	85	85	85
Hydrogen tank capacity (m^3)	1000	1000	1000	1000
Initial capacity of gas tank (%)	30	30	30	30
Hydrogen tank cost (£/m^3)	27.63	27.63	27.63	27.63
Tank storage efficiency (%)	95	95	95	95
Electric to gas efficiency (%)	75	75	75	75
Electricity-to-gas coefficient (kWh/m^3)	0.2	0.2	0.2	0.2
Fuel cell generator capacity (kW)	800	1500	1000	1200
Gas-to-electric efficiency (%)	65	65	65	65
Gas-to-electricity coefficient (m^3/kWh)	0.295	0.295	0.295	0.295
RE feed-in tariff (£/kWh)	0.03	0.03	0.03	0.03

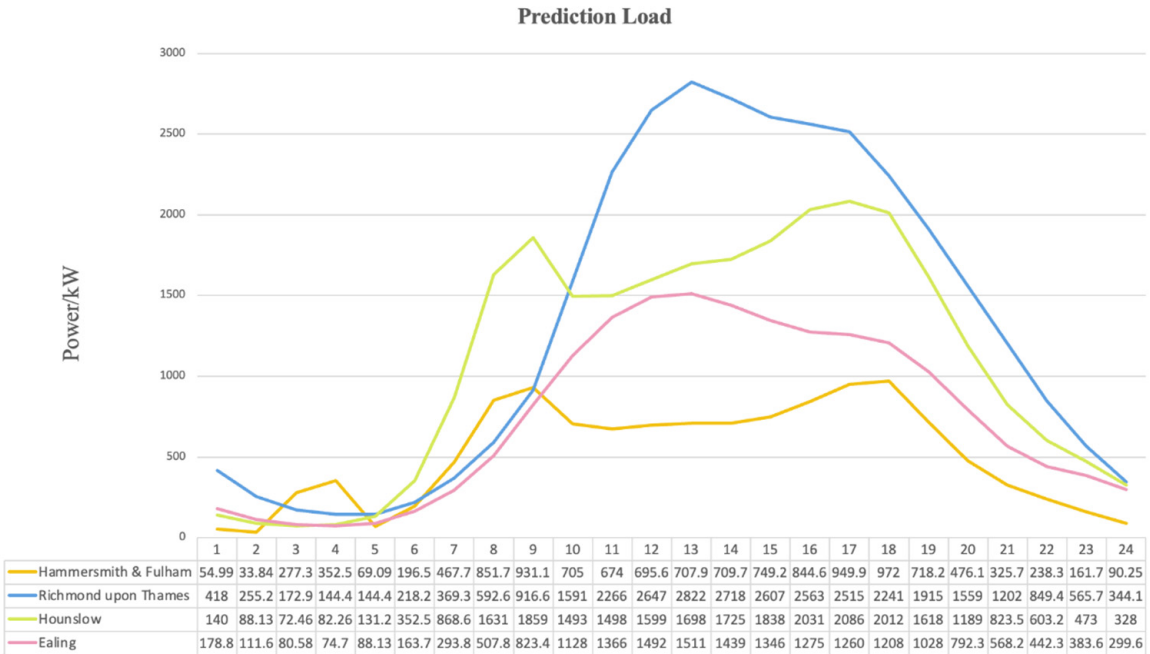

	1	2	3	4	5	6	7	8	9	10	11	12	13	14	15	16	17	18	19	20	21	22	23	24
Hammersmith & Fulham	54.99	33.84	277.3	352.5	69.09	196.5	467.7	851.7	931.1	705	674	695.6	707.9	709.7	749.2	844.6	949.9	972	718.2	476.1	325.7	238.3	161.7	90.25
Richmond upon Thames	418	255.2	172.9	144.4	144.4	218.2	369.3	592.6	916.6	1591	2266	2647	2822	2718	2607	2563	2515	2241	1915	1559	1202	849.4	565.7	344.1
Hounslow	140	88.13	72.46	82.26	131.2	352.5	868.6	1631	1859	1493	1498	1599	1698	1725	1838	2031	2086	2012	1618	1189	823.5	603.2	473	328
Ealing	178.8	111.6	80.58	74.7	88.13	163.7	293.8	507.8	823.4	1128	1366	1492	1511	1439	1346	1275	1260	1208	1028	792.3	568.2	442.3	383.6	299.6

Figure 6. SHS-EVCSs prediction load using [56] method.

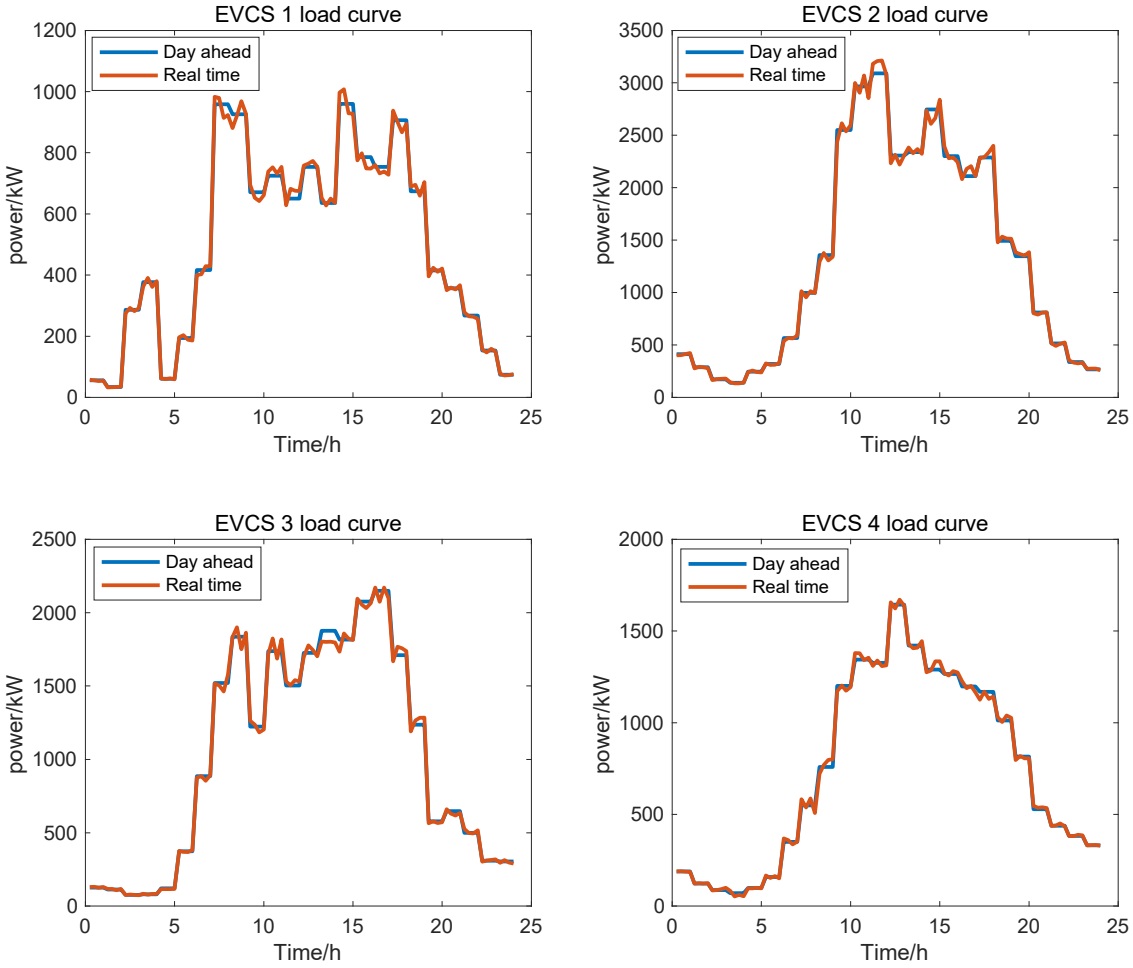

Figure 7. SHS-EVCSs day ahead and real-time load curve without TOU strategy.

Figure 8 shows the anticipated EV load and the impact of implementing a TOU strategy. The blue curve is the standard EV charging pattern without TOU modifications, with pronounced peaks for SHS-EVCSs 1 and 3 around 9 a.m. and 7 p.m.—times that align with typical charging periods. During the early hours (0 to 5 a.m.), power demand is notably lower. In contrast, SHS-EVCSs 2 and 4 experience their peak loads at noon, with lower demand levels mirroring those of SHS-EVCSs 1 and 3. The orange curve, indicating post-TOU implementation, shows a significant smoothing of peaks across all SHS-EVCSs, confirming the strategy's effectiveness in peak shaving. Notably, SHS-EVCSs 2 and 4 exhibit a singular peak at noon, and the mean absolute percentage error (MAPE) for this is 11.37% and 13.56%, further validating the efficiency of the TOU approach. The benefits of the TOU strategy include a substantial decrease in peak loads, visible in the shift from the blue to the orange curve, which alleviates stress on the electrical grid. This could reduce the need for further grid infrastructure enhancements and diminish electricity costs. By more evenly distributing power consumption, the TOU strategy enhances the operational efficiency of power generation and distribution networks, contributing to more consistent grid performance. Furthermore, this strategy can yield financial savings for both utility providers and consumers by minimizing the dependence on more costly and environmentally unfriendly peak power generation.

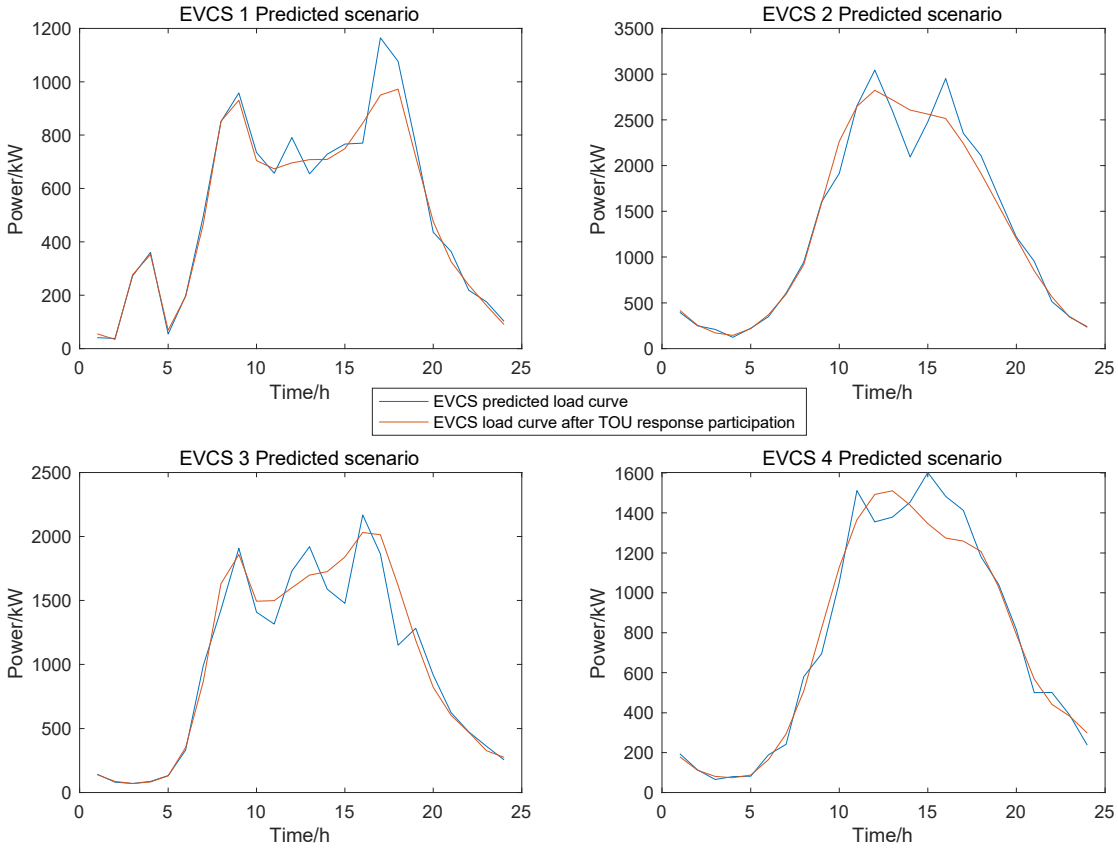

Figure 8. EV prediction load and load after demand side management.

Figure 9 shows the prediction and reduced scenarios for SHS-EVCS prediction. For each SHS-EVCS, a total of 50 scenarios were predicted. In the scenario reduction process, there is a need to identify a subset of the initial scenario set and reassign probabilities to these retained scenarios. This reassignment aims to minimize the probabilistic distance between the probability distribution of the retained scenarios and the initial scenario set.

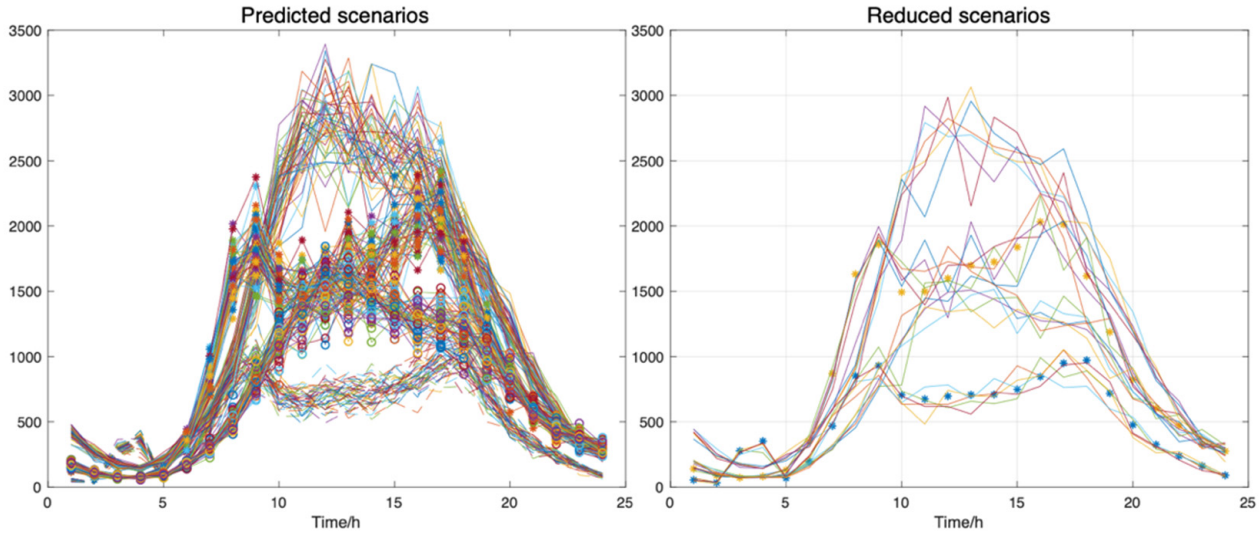

Figure 9. Prediction scenarios and reduced scenarios.

To identify the scenario with the smallest probability to be reduced, one scenario is removed after each iteration. By the end of the entire iterative process, at least the five scenarios with the highest probabilities are retained by the end of the total iteration. This method ensures that while the number of scenarios is reduced, the most representative scenarios are preserved, thereby maintaining the key probabilistic characteristics of the initial scenario set. This approach significantly reduces computational complexity while accurately reflecting the statistical properties of the initial scenario set. Over the span of a day, the prediction scenarios display a high level of variation and complexity, with numerous intersecting lines and extraneous data. In contrast, the reduced scenarios offer a clearer, more focused view, emphasizing the primary trends in electricity demand. Notably, peak demand times at 9 a.m. and 6 p.m. are clear in both scenarios. However, the streamlined scenarios strip away minor variations and outliers, thereby simplifying the information and enhancing its applicability for strategic decision-making.

5. Results and Discussion

Figure 10 shows the EV traffic flow for each SHS-EVCS over a 24 h period, highlighting distinct peaks and valleys in demand. The most significant peak occurs around 10 a.m., with all stations experiencing a marked increase in EV numbers, signalling a morning rush. EVCS 2 sees the highest vehicle count during this period, likely due to its location in a commercial area, making it a popular choice for morning charging. In contrast, EVCS 3, although less busy overall, has notable peaks at 6 a.m. and 9 a.m., indicating specific times of high demand. Another notable surge in charging activity is observed at 8 p.m., aligning with evening charging routines. This pattern is consistent across all stations, with each experiencing an increase in vehicle numbers during this time. EVCS 4 also shows a significant evening peak, indicating steady demand during these hours. The early hours from midnight to 5 a.m. show the lowest vehicle numbers, suggesting minimal charging activity. This low level of activity during the early morning hours might reflect reduced travel and charging demand, potentially due to effective TOU strategies that shift usage away from these times.

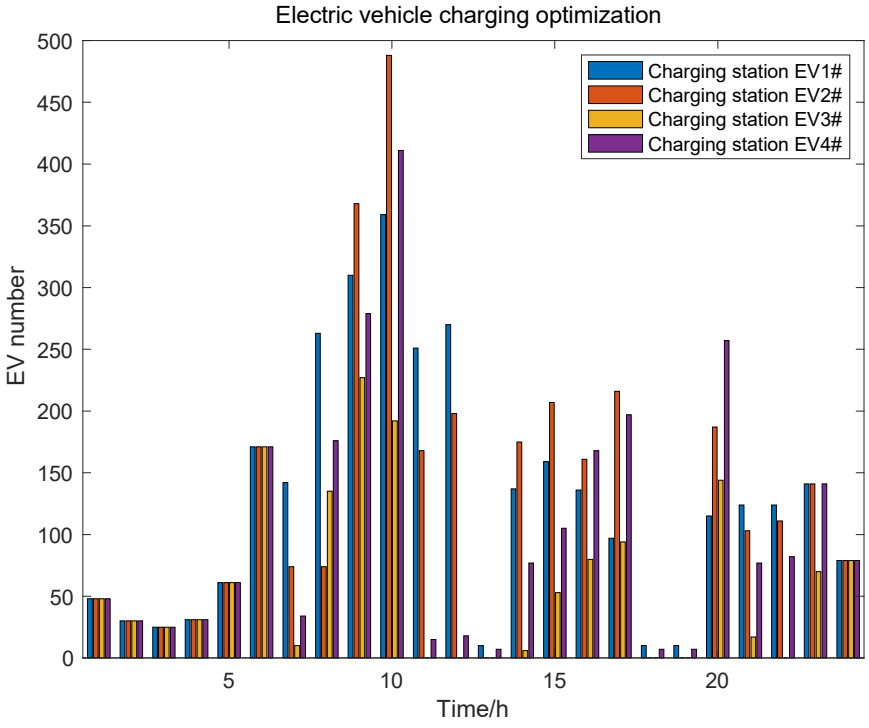

Figure 10. EV charging number optimization.

The charging trends observed are typically linked to daily routines, with morning peaks aligning with pre-work charging and evening peaks with post-work charging. Most EV drivers prefer charging their vehicles before and after work. By adopting strategies to manage these peak times, such as expanding charging station capacity or fine-tuning charging schedules, the efficiency of the entire system and the user experience can be significantly improved.

Figures 11–14 show the energy consumption and electricity load profiles for four SHS-EVCSs. Throughout the daytime, PV systems serve as the main electricity source due to their efficiency and sustainability, making them well-suited for daytime energy production. This reduces reliance on grid-supplied electricity and helps to lower carbon emissions. The use of solar power not only cuts operational costs but also supports broader RE initiatives. With the setting of the sun and the cessation of solar energy production, the SHS-EVCSs transition to using hydrogen fuel cells for power generation. The hydrogen used is typically produced during periods of low demand or when there is surplus solar energy, contributing to a sustainable and reliable energy supply. Additionally, these systems are supplemented by battery storage that accumulates excess energy produced during daylight hours, particularly from the PV systems and the electricity purchased from the grid when its buying price is lower than the P2P purchase price. These batteries then discharge power during peak usage times or when the production from renewable sources is reduced, thereby ensuring a consistent and dependable electricity supply. This capability to balancing the variability of renewable sources underscores the importance of battery integration in maintaining energy stability.

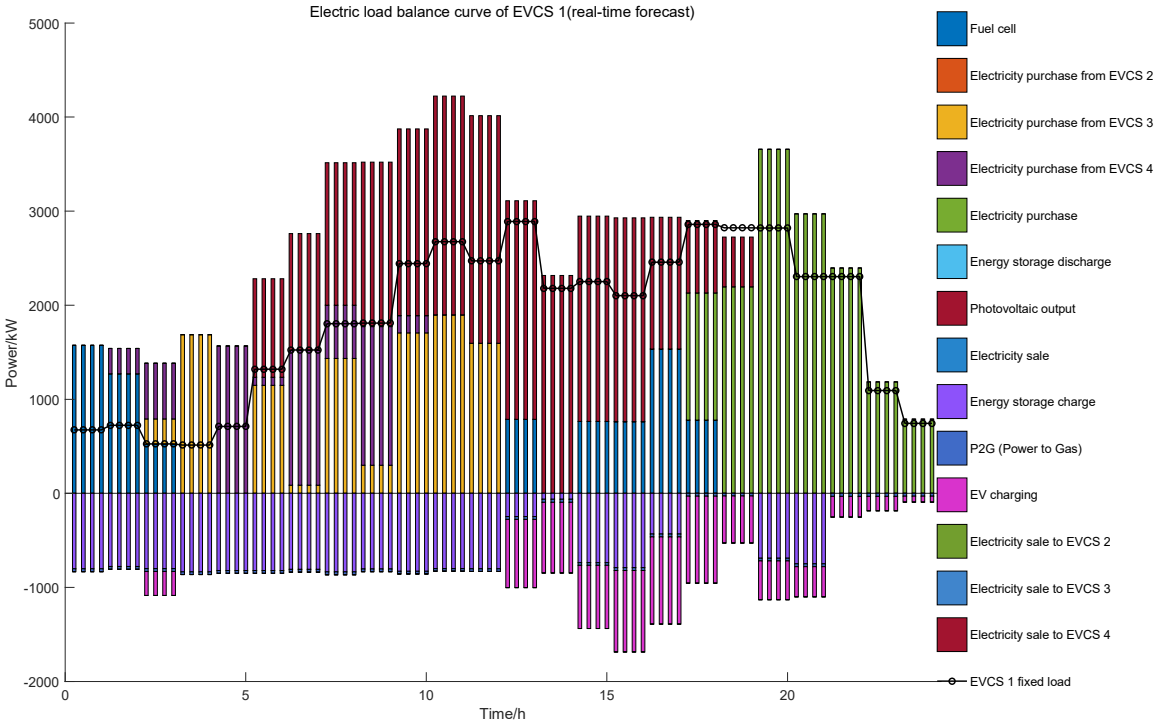

Figure 11. SHS-EVCS1 RE usage and electricity load curve.

Moreover, each SHS-EVCS can engage in electricity trading with other stations in the network, aimed at minimizing costs. This practice of inter-station energy trading enhances flexibility and efficiency in energy management, allowing each station to optimize its operations and reduce expenses. With diverse energy sources and trading options, the SHS-EVCSs are well-equipped to respond to changing energy demands and market conditions, thereby improving the overall stability and sustainability of the electrical grid.

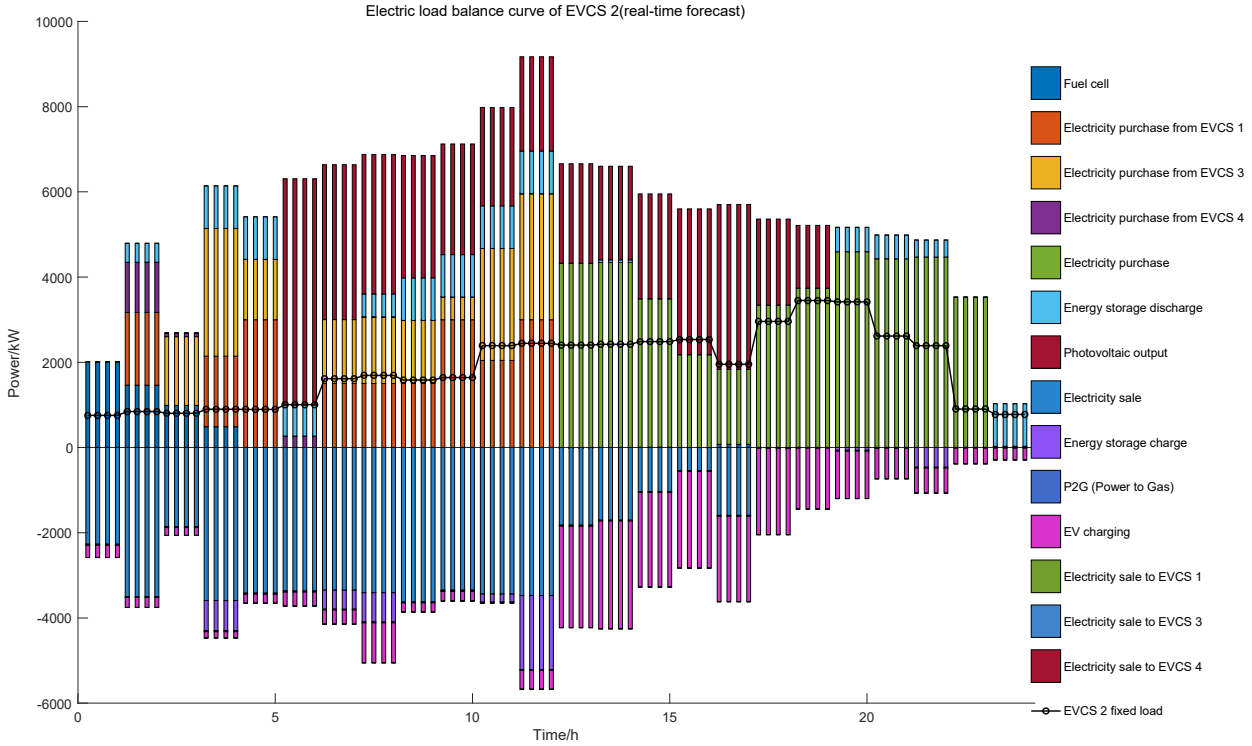

Figure 12. SHS-EVCS2 RE usage and electricity load curve.

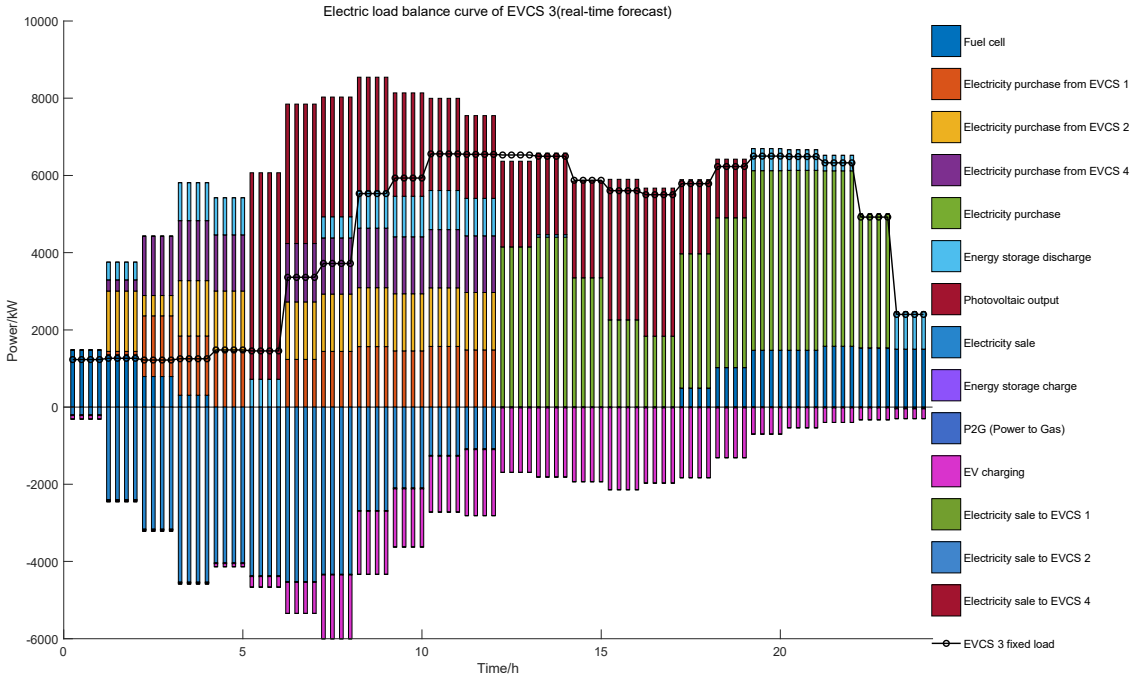

Figure 13. SHS-EVCS3 RE usage and electricity load curve.

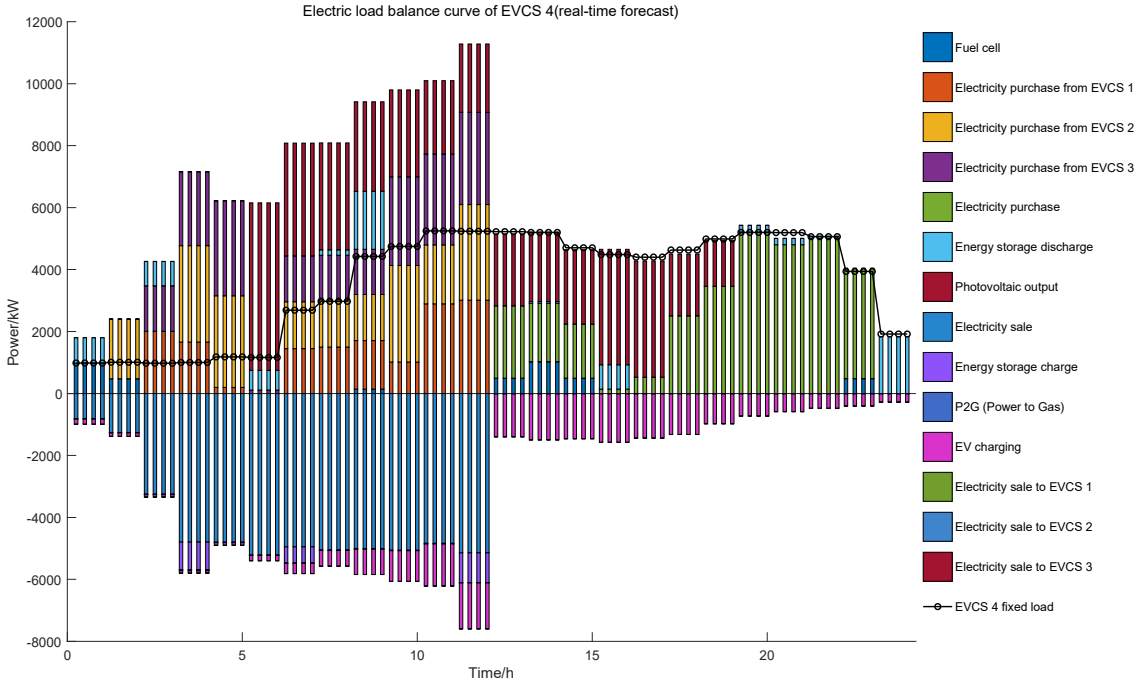

Figure 14. SHS-EVCS4 RE usage and electricity load curve.

Figure 15 shows the relationship between electricity prices and social welfare over 24 h. Initially, the electricity price is relatively high, at around £0.40. The price drops significantly from 11 a.m. to 11 p.m. and remains low, hovering around £0.20. After 11 p.m., the price rises again, peaking at approximately £0.35. Social welfare trends start at a low level when the electricity price is high. As the electricity price decreases, social welfare increases, indicating an inverse relationship between the two variables. This inverse relationship is especially noticeable between 3 p.m. and 11 p.m. when lower electricity prices correspond with higher and more stable levels of social welfare. This relationship suggests that lower electricity prices contribute to higher social welfare, likely due to more affordable energy access benefiting consumers and overall societal well-being. In the economic market, price fluctuations in electricity can be attributed to changes in demand and supply, peak and off-peak hours, or other market dynamics. However, in this paper, the fluctuations in electricity prices are due to the SHS-EVCSs coalition. These fluctuations impact social welfare, but the general trend indicates that as electricity prices decrease, social welfare stabilizes and increases slightly.

Figure 16 shows the relationship between social welfare and time across intervals (day 1, day 2, and day 3). The consistent patterns observed across these scenarios suggest that short-term forecasting can be nearly as effective as long-term forecasting for immediate social welfare planning. This provides insight into the relationship between various time horizon scenarios and social welfare in energy management.

Figure 17 depicts the optimal dynamic power load over 24 h. During the valley load period, from 11 p.m. to 9 a.m., the power load increases from approximately 4000 kW to 13,000 kW. The charging demand for EVs is low during this time, as some drivers charge their EVs at home, and some EVs are already fully charged or have stopped charging. From 6 a.m. to 7 a.m., the sharp increase in load likely indicates that most EV drivers are charging their vehicles as they prepare to leave for work. The SHS-EVCS optimizes the EV charging load through demand response, load forecasting algorithms, and TOU pricing, enhancing power utilization and balancing the internal grid load. It also regulates power distribution to avoid resource wastage during the valley period. At 10 a.m. and from 4 p.m. to 5 p.m., the power load stabilizes around 14,000 kW. During these times, the charging demand for

EVs is relatively stable. Dynamic pricing strategies can further smoothen the load curve and reduce grid pressure fluctuations.

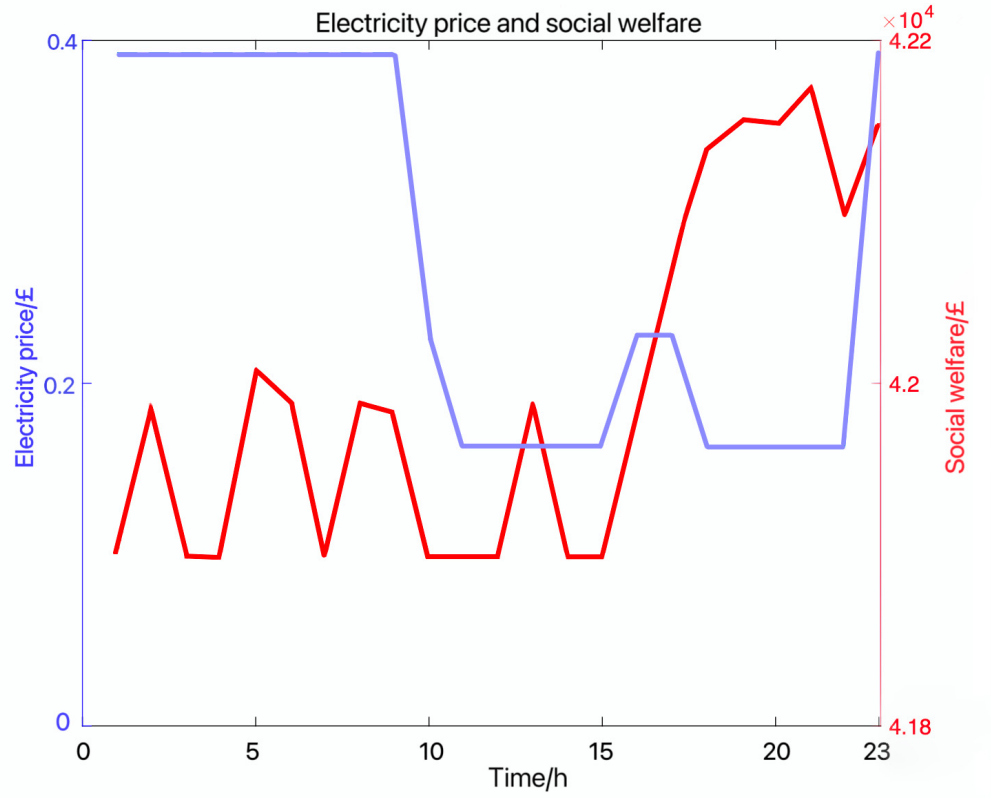

Figure 15. Electricity price and social welfare.

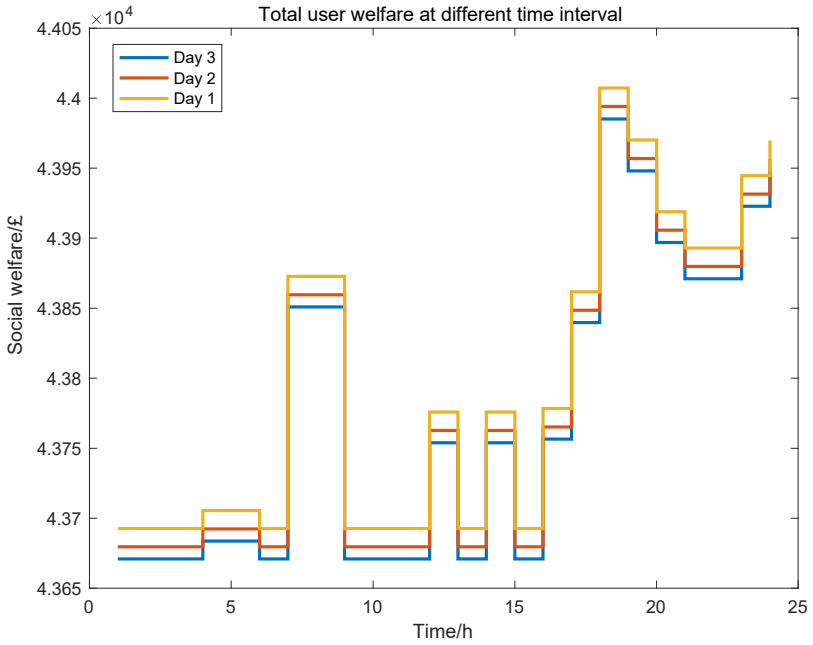

Figure 16. Total user welfare at different time intervals.

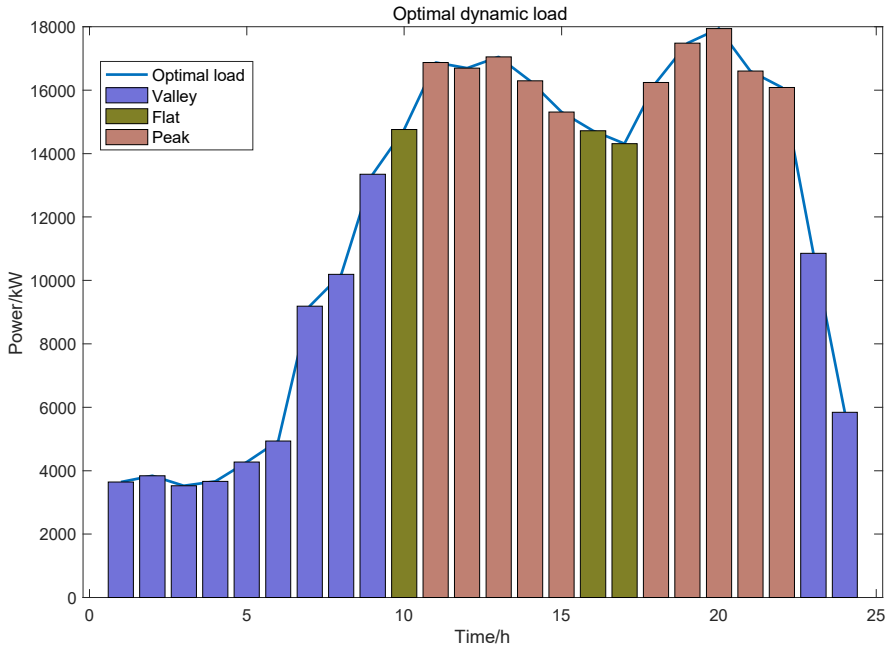

Figure 17. Total optimal dynamic load.

Peak load periods occur from 11 a.m. to 3 p.m. and 6 p.m. to 10 p.m., with loads exceeding 16,000 kW and peaking at 18,000 kW. During these times, the charging demand for EVs rises sharply, especially in the evening when many drivers charge their EVs after returning home from work. Peak shaving strategies such as time-based charging fees, restrictions, and intelligent scheduling systems can be adopted to address this situation. Adjusting the output power of charging stations and coordinating power demand can reduce the grid pressure during peak periods. Additionally, SHS-EVCSs utilize energy storage systems to feed excess power back into the grid during peak times, effectively achieving peak shaving and valley filling. Combined with the IMS, this enables the real-time monitoring and dynamic management of EV charging demand, further enhancing the reliability and stability of both internal and external grids.

Figure 18 shows the profit versus iteration, with iterations ranging from 0 to 25 and profit values from £0 to £18,000. The profit rapidly increases from iteration 1 to 2, reaching approximately £16,800, and then stabilizes around this value for all subsequent iterations. This indicates that this process achieves optimal profit quickly, with minimal changes needed afterward. The initial setup or optimization has an important impact, suggesting that focusing resources on this phase is crucial.

Table 3 presents the energy storage and generation technologies across Hammersmith & Fulham, Richmond upon Thames, Hounslow, and Ealing. Several trends and strategic differences are evident in the deployment of battery storage systems and hydrogen storage systems. The analysis reveals that Ealing has the highest battery storage capacity at 2000 kWh. In contrast, Richmond upon Thames shows a more diversified approach, with significant investments across all technologies. Richmond highlights the highest expenditures in battery systems, with a capacity of 1762.6758 kWh at a cost of £584,415.16, and fuel cell capacity at 1988 kWh costing £997,260.32. All areas have hydrogen storage system capacities of around 1300–1500 kWh. However, Richmond upon Thames again stands out with a slightly higher capacity and cost. Richmond's investment in fuel cells is particularly notable, possibly due to their efficiency and operational flexibility benefits compared to other forms of energy storage and generation. Ealing and Hounslow, while also investing substantially, have lesser capacities and costs associated with their fuel cells.

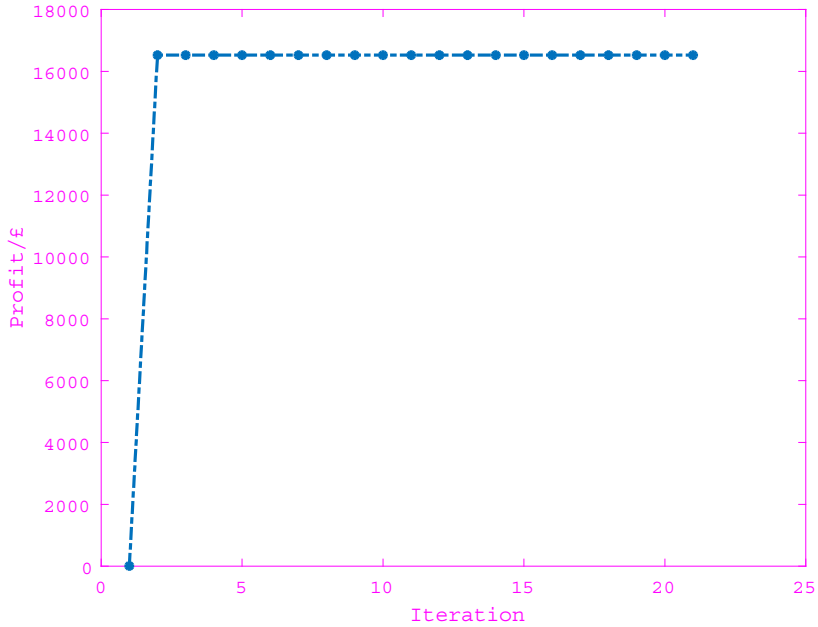

Figure 18. Convergence of real-time electricity price distributed (SHS-EVCS profit) algorithms.

Table 3. Energy optimal parameters and cost.

Parameters	Hammersmith & Fulham	Richmond upon Thames	Hounslow	Ealing
Battery storage system (kWh)	800	1762.68	1000	2000
Battery storage system investment and O/M cost (£/kWh)	265,240	584,415.16	497,330	663,100
Hydrogen storage tank capacity (kWh)	1369.49	1524.98	1379.16	1277.06
Hydrogen storage tank investment and O/M cost (£/kWh)	55,100.09	61,356.08	55,489.2	51,381.16
Fuel cell (kWh)	1582.5	1988	1500	1000
Fuel cell investment and O/M cost (£/kWh)	793,845.3	997,260.32	752,460	501,640

The Table 4 shows the MAPE for four areas, Hammersmith & Fulham (13.04%), Richmond upon Thames (11.37%), Hounslow (11.8%), and Ealing (13.56%). Richmond upon Thames has the lowest MAPE, indicating the highest prediction accuracy, closely followed by Hounslow. Hammersmith & Fulham and Ealing have higher MAPE values, with Ealing having the highest, indicating the least accurate predictions. Overall, while these values are within a reasonable and good range, there is a need for improved forecasting methods in the future.

Table 4. MAPE for 4 SHS-EVCSs.

	Hammersmith & Fulham	Richmond upon Thames	Hounslow	Ealing
MAPE/%	13.04	11.37	11.8	13.56

6. Conclusions

Incorporating a Markov decision process to model EV charging times and using Monte Carlo simulations to predict charging demand has been instrumental in capturing the stochastic nature of EV usage patterns. These methodologies provide a high degree of accuracy in forecasting, enabling the optimization model to adapt to varying conditions and enhancing the reliability of the SHS-EVCS system. Applying the dual theory to determine

real-time electricity prices also helps manage demand-side energy consumption. The system can incentivize off-peak charging, reduce peak load stress, and contribute to grid stability by leveraging these theoretically optimal prices. This aligns with broader demand-side management goals, achieving peak shaving and valley filling, reducing overall energy costs, and improving system sustainability. Empirical analysis and case studies demonstrate the effectiveness of TOU strategies in peak load reduction and load balancing. Comparative results between predicted and actual load scenarios highlight the significant impact of TOU in mitigating demand spikes and promoting efficient energy utilization. This benefits the power grid by reducing the need for additional infrastructural investments and offers economic advantages to both EVCS operators and consumers through lower electricity prices and operational costs.

In conclusion, integrating advanced optimization techniques and game theory models in managing SHS-EVCS systems offers a promising pathway toward sustainable and efficient energy infrastructure. The findings of this paper offer valuable insights into the complex interactions between renewable energy sources, storage systems, and EV charging demands. Social welfare could reach up to £4.218×10^4 if the EV charging electricity price is below £0.20. Future research should continue to explore the scalability of these models and their application in diverse geographical and economic contexts, thereby contributing to the global transition toward cleaner and more resilient energy systems.

Author Contributions: Conceptualization, L.D., G.T. and C.S.L.; methodology, L.D. and C.S.L.; software, L.D.; validation, L.D.; formal analysis, L.D.; investigation, L.D.; resources, L.D.; data curation, L.D.; writing—original draft preparation, L.D.; writing—review and editing, L.D., C.S.L. and G.T.; visualization, L.D.; supervision, C.S.L. and G.T.; project administration, C.S.L. and G.T. All authors have read and agreed to the published version of the manuscript.

Funding: This research is supported by Oracle for Research Grant (3146375).

Data Availability Statement: The original contributions presented in the study are included in the article, further inquiries can be directed to the corresponding author.

Conflicts of Interest: The authors declare no conflicts of interest.

Nomenclature

a_f	Waiting probability
a_k^h	The downward direction of function $A(\lambda_k)$
B_{cap}	Battery capacity, 60 kWh (Tesla model 6 battery capacity)
c_f, d_f	The charging probability and the probability of interrupted charging
$C_k(G_k)$	The cost of SHS-EVCS to provide electricity for G_k at time k
C_k	The capital and O&M cost for SHS-EVCS from first-level output
D	Total driver
E_{km}	Energy consumption, 16.25 kWh/100 km
EVC_f, EVD_f	The states of charging mode and wating mode
f_{max}	Maximum number of discrete variables
$\Delta(-f)$	The electricity loss when driving the EV
G_k	SHS-EVCS's electricity supply at time k
G_k^{min}, G_k^{max}	Minimum and maximum electricity supplies of SHS-EVCS
m_d^k, M_d^k	Minimum and maximum electricity consumptions of EV driver d at time k
N_{ev}	Total EV number
p_{ij}, p_{ji}	Transition probability of state i to j, transition probability of state j to i
$P_s(EVC_f)$, $P_s(EVD_f)$	The state probability of EVC_f and EVD_f
P_c	Fixed charging power, 7 kW

$P_{cha,sum}$	Total charging power
$P_{cha,i}$	$i'th$ EV charging power
s_f^{dis}	The $f'th$ discrete state
S^{dis}	Discrete state space
SoC_{start}, $SoC_{start,max}$, $SoC_{start,min}$	Initial, maximum, and minimum SoCs for EV
ΔT_1, ΔT_2	Charging and waiting times
v	Average driving speed, 32 km/h
$V_d\left(x_d^k,\ \omega_d^k\right)$	Utility of EV driver d using x_d^k at time k
x_f^{dis}	The $f'th$ discrete variable
x_d^k	The electricity consumption of EV driver d at time k
ω_d^k	Driver d's elasticity of charging his EV at time k, $\omega_d^k \in [1,\ 3.5]$
η_c	EV battery efficiency, 95%
λ_k	The real-time electricity price
γ_k^h	The distance, 0.8

Abbreviations

CSs	Charging stations
DR	Demand response
DSM	Demand-side management
EV	Electric vehicle
G2P	Gas to power
IMS	Internal Management System
MAPE	Mean Absolute Percentage Error
P2G	Power to gas
PV	Photovoltic
RE	Renewable energy
SHS-EVCSs	Solar–Hydrogen-Battery Storage Electric Vehicle Charging Stations

References

1. Liu, C.; Chau, K.T.; Wu, D.; Gao, S. Opportunities and Challenges of Vehicle-to-Home, Vehicle-to-Vehicle, and Vehicle-to-Grid Technologies. *Proc. IEEE* **2013**, *101*, 2409–2427. [CrossRef]
2. Kubański, M. Prospects for the Use of Electric Vehicles in Public Transport on the Example of the City of Czechowice-Dziedzice. *Transp. Res. Procedia* **2020**, *44*, 110–114. [CrossRef]
3. Zeng, J.; Li, M.; Liu, J.F.; Wu, J.; Ngan, H.W. Operational optimization of a stand-alone hybrid renewable energy generation system based on an improved genetic algorithm. In Proceedings of the 2010 IEEE Power and Energy Society General Meeting, Providence, RI, USA, 25–29 July 2010.
4. Tushar, W.; Yuen, C.; Huang, S.; Smith, D.B.; Poor, H.V. Cost Minimization of Charging Stations with Photovoltaics: An Approach With EV Classification. *IEEE Trans. Intell. Transp. Syst.* **2016**, *17*, 156–169. [CrossRef]
5. Keyhani, A. *Design of Smart Power Grid Renewable Energy Systems*; John Wiley & Sons: Hoboken, NJ, USA, 2019; pp. 1–606. [CrossRef]
6. Das, H.S.; Rahman, M.M.; Li, S.; Tan, C.W. Electric vehicles standards, charging infrastructure, and impact on grid integration: A technological review. *Renew. Sustain. Energy Rev.* **2019**, *120*, 109618. [CrossRef]
7. Bohnsack, R.; Pinkse, J.; Kolk, A. Business models for sustainable technologies: Exploring business model evolution in the case of electric vehicles. *Res. Policy* **2014**, *43*, 284–300. [CrossRef]
8. Markkula, J.; Rautiainen, A.; Jarventausta, P. The business case of electric vehicle quick charging–no more chicken or egg problem. *World Electr. Veh. J.* **2013**, *6*, 921–927. [CrossRef]
9. Madina, C.; Zamora, I.; Zabala, E. Methodology for assessing electric vehicle charging infrastructure business models. *Energy Policy* **2015**, *89*, 284–293. [CrossRef]
10. Ehteshami, S.M.M.; Chan, S.H. The role of hydrogen and fuel cells to store renewable energy in the future energy network–potentials and challenges. *Energy Policy* **2014**, *73*, 103–109. [CrossRef]
11. Yue, M.; Lambert, H.; Pahon, E.; Roche, R.; Jemei, S.; Hissel, D. Hydrogen energy systems: A critical review of technologies, applications, trends and challenges. *Renew. Sustain. Energy Rev.* **2021**, *146*, 111180. [CrossRef]
12. Yap, K.Y.; Chin, H.H.; Klemeš, J.J. Solar Energy-Powered Battery Electric Vehicle charging stations: Current development and future prospect review. *Renew. Sustain. Energy Rev.* **2022**, *169*, 112862. [CrossRef]

13. Barman, P.; Dutta, L.; Bordoloi, S.; Kalita, A.; Buragohain, P.; Bharali, S.; Azzopardi, B. Renewable energy integration with electric vehicle technology: A review of the existing smart charging approaches. *Renew. Sustain. Energy Rev.* **2023**, *183*, 113518. [CrossRef]
14. Manousakis, N.M.; Karagiannopoulos, P.S.; Tsekouras, G.J.; Kanellos, F.D. Integration of Renewable Energy and Electric Vehicles in Power Systems: A Review. *Processes* **2023**, *11*, 1544. [CrossRef]
15. Rajendran, G.; Vaithilingam, C.A.; Misron, N.; Naidu, K.; Ahmed, R. A comprehensive review on system architecture and international standards for electric vehicle charging stations. *J. Energy Storage* **2021**, *42*, 103099. [CrossRef]
16. Jauhar, S.K.; Sethi, S.; Kamble, S.S.; Mathew, S.; Belhadi, A. Artificial intelligence and machine learning-based decision support system for forecasting electric vehicles' power requirement. *Technol. Forecast. Soc. Change* **2024**, *204*, 123396. [CrossRef]
17. Thompson, L.; Davidson, P. Future of Battery Storage: Impact of Solid-State Technology on EV Charging Stations. *Energy Storage Trends* **2023**, *7*, 99–115.
18. Ali, A.; Shakoor, R.; Raheem, A.; Abd Muqeet, H.A.; Awais, Q.; Khan, A.A.; Jamil, M. Latest energy storage trends in multi-energy standalone electric vehicle charging stations: A comprehensive study. *Energies* **2022**, *15*, 4727. [CrossRef]
19. Franco, A.; Giovannini, C. Recent and Future Advances in Water Electrolysis for Green Hydrogen Generation: Critical Analysis and Perspectives. *Sustainability* **2023**, *15*, 16917. [CrossRef]
20. Boglou, V.; Karavas, C.-S.; Karlis, A.; Arvanitis, K.G.; Palaiologou, I. An Optimal Distributed RES Sizing Strategy in Hybrid Low Voltage Networks Focused on EVs Integration. *IEEE Access* **2023**, *11*, 16250–16270. [CrossRef]
21. Mitali, J.; Dhinakaran, S.; Mohamad, A.A. Energy Storage Systems: A Review. *Energy Storage Sav.* **2022**, *1*, 166–216. [CrossRef]
22. Huang, H.; Deng, L.; Zhang, L. Review of Real-time Pricing based on Demand Response. *Electr. Technol.* **2015**, *16*, 1–6.
23. Deng, R.; Yang, Z.; Chow, M. A survey on demand response in smart grids: Mathematical models and approaches. *IEEE Trans. Ind. Inform.* **2015**, *11*, 570–582. [CrossRef]
24. Palensky, P.; Dietrich, D. Demand side management: Demand response, intelligent energy systems, and smart loads. *IEEE Trans. Ind. Inform.* **2011**, *7*, 381–388. [CrossRef]
25. Mariano-Hernández, D.; Hernández-Callejo, L.; Zorita-Lamadrid, A.; Duque-Pérez, O.; García, F.S. A review of strategies for building energy management system: Model predictive control, demand side management, optimization, and fault detect & diagnosis. *J. Build. Eng.* **2020**, *33*, 101692. [CrossRef]
26. Onile, A.E.; Machlev, R.; Petlenkov, E.; Levron, Y.; Belikov, J. Uses of the digital twins concept for energy services, intelligent recommendation systems, and demand side management: A review. *Energy Rep.* **2021**, *7*, 997–1015. [CrossRef]
27. Demand Response as Low-Cost Reliability Service: Techno-Economic Benefits and Challenges. Available online: https://smartgrid.ieee.org/newsletters/november-2017/1070-demand-response-as-low-cost-reliability-service-techno-economic-benefits-and-challenges (accessed on 30 November 2017).
28. Paterakis, N.G.; Erdinç, O.; Catalão, J.P.S. An overview of demand response: Key-elements and international experience. *Renew. Sustain. Energy Rev.* **2017**, *69*, 871–891. [CrossRef]
29. Märkle-Huß, J.; Feuerriegel, S.; Neumann, D. Large-scale demand response and its implications for spot prices, load and policies: Insights from the German-Austrian electricity market. *Appl. Energy* **2018**, *210*, 1290–1298. [CrossRef]
30. Zhu, H.; Gao, Y.; Hou, Y. Real-Time Pricing for Demand Response in Smart Grid Based on Alternating Direction Method of Multipliers. *Math. Probl. Eng.* **2018**, *2018*, 1–10. [CrossRef]
31. Pfeifer, A.; Dobravec, V.; Pavlinek, L.; Krajačić, G.; Duić, N. Integration of renewable energy and demand response technologies in interconnected energy systems. *Energy* **2018**, *161*, 447–455. [CrossRef]
32. Mimica, M.; Sinovčić, Z.; Jokić, A.; Krajačić, G. The role of the energy storage and the demand response in the robust reserve and network-constrained joint electricity and reserve market. *Electr. Power Syst. Res.* **2022**, *204*, 107716. [CrossRef]
33. Lu, R.; Hong, S.H.; Zhang, X. A Dynamic pricing demand response algorithm for smart grid: Reinforcement learning approach. *Appl. Energy* **2018**, *220*, 220–230. [CrossRef]
34. Asadi, G.; Gitizadeh, M.; Roosta, A. Welfare maximization under real-time pricing in smart grid using PSO algorithm. In Proceedings of the 2013 21st Iranian Conference on Electrical Engineering (ICEE), Mashhad, Iran, 14–16 May 2013; pp. 1–7. [CrossRef]
35. Samadi, P.; Mohsenian-Rad, H.; Schober, R.; Wong, V.W.S. Advanced demand side management for the future smart grid using mechanism design. *IEEE Trans. Smart Grid* **2012**, *3*, 1170–1180. [CrossRef]
36. Fu, Z.; He, X.; Huang, T.; Abu-Rub, H. A distributed continuous time consensus algorithm for maximize social welfare in micro grid. *J. Frankl. Inst.* **2016**, *353*, 3966–3984. [CrossRef]
37. Shafiei, M.; Ghasemi-Marzbali, A. Electric vehicle fast charging station design by considering probabilistic model of renewable energy source and demand response. *Energy* **2023**, *267*, 126545. [CrossRef]
38. Meng, W.; Song, D.; Huang, L.; Chen, X.; Yang, J.; Dong, M.; Talaat, M.; Elkholy, M.H. Distributed energy management of electric vehicle charging stations based on hierarchical pricing mechanism and aggregate feasible regions. *Energy.* **2024**, *291*, 130332. [CrossRef]
39. Huang, X.; Lin, Y.; Lim, M.K.; Zhou, F.; Liu, F. Electric vehicle charging station diffusion: An agent-based evolutionary game model in complex networks. *Energy* **2022**, *257*, 124700. [CrossRef]
40. Li, G.; Yang, J.; Hu, Z.; Zhu, X.; Xu, J.; Sun, Y.; Zhan, X.; Wu, F. A novel price-driven energy sharing mechanism for charging station operators. *Energy Econ.* **2023**, *118*, 106518. [CrossRef]

41. Wu, Y.; Ravey, A.; Chrenko, D.; Miraoui, A. Demand side energy management of EV charging stations by approximate dynamic programming. *Energy Convers. Manag.* **2019**, *196*, 878–890. [CrossRef]
42. Adetunji, K.E.; Hofsajer, I.W.; Abu-Mahfouz, A.M.; Cheng, L. An optimization planning framework for allocating multiple distributed energy resources and electric vehicle charging stations in distribution networks. *Appl. Energy* **2022**, *322*, 119513. [CrossRef]
43. Abid, S.; Ahshan, R.; Al Abri, R.; Al-Badi, A.; Albadi, M. Techno-economic and environmental assessment of renewable energy sources, virtual synchronous generators, and electric vehicle charging stations in microgrids. *Appl. Energy* **2024**, *35*, 122028. [CrossRef]
44. Güven, A.F. Integrating electric vehicles into hybrid microgrids: A stochastic approach to future-ready renewable energy solutions and management. *Energy* **2024**, *303*, 131968. [CrossRef]
45. Duan, L.; Guo, Z.; Taylor, G.; Lai, C.S. Multi-Objective Optimization for Solar-Hydrogen-Battery-Integrated Electric Vehicle Charging Stations with Energy Exchange. *Electronics* **2023**, *12*, 4149. [CrossRef]
46. Duan, L.; Yuan, Y.; Taylor, G.; Lai, C.S. Game-Theory-Based Design and Analysis of a Peer-to-Peer Energy Exchange System between Multi-Solar-Hydrogen-Battery Storage Electric Vehicle Charging Stations. *Electronics* **2024**, *13*, 2392. [CrossRef]
47. Ma, Q.; Tong, X.; Huang, J.; Wang, P.; Li, J. Nodal charging demand forecast of EVs considering drivers’ psychological bearing ability based on NMC-MCS. *IET Gener. Transm. Distrib.* **2021**, *16*, 467–478. [CrossRef]
48. Fotouhi, Z.; Hashemi, M.R.; Narimani, H.; Bayram, I.S. A General Model for EV Drivers Charging Behavior. *IEEE Trans. Veh. Technol.* **2019**, *68*, 7368–7382. [CrossRef]
49. Tan, J.; Wang, L. Real-Time Charging Navigation of Electric Vehicles to Fast Charging Stations: A Hierarchical Game Approach. *IEEE Trans. Smart Grid* **2015**, *8*, 846–856. [CrossRef]
50. Deilami, S.; Masoum, A.S.; Moses, P.S.; Masoum, M.A.S. Real-Time Coordination of Plug-In Electric Vehicle Charging in Smart Grids to Minimize Power Losses and Improve Voltage Profile. *IEEE Trans. Smart Grid* **2011**, *2*, 456–467. [CrossRef]
51. Electric Vehicle Charging Research Survey with Electric Vehicle Drivers Research Report. Department of Transportation. 2022. Available online: https://assets.publishing.service.gov.uk/media/628f5603d3bf7f037097bd73/dft-ev-driver-survey-summary-report.pdf (accessed on 30 April 2022).
52. Samadi, P.; Mohsenian-Rad, A.-H.; Schober, R.; Wong, V.W.S.; Jatskevich, J. Optimal real-time pricing algorithm based on utility maximization for smart grid. In Proceedings of the 2010 First IEEE International Conference on Smart Grid Communications, Gaithersburg, MD, USA, 4–6 October 2010; pp. 415–420. [CrossRef]
53. Mohsenian-Rad, A.-H.; Wong, V.W.S.; Jatskevich, J.; Schober, R.; Leon-Garcia, A. Autonomous demand-side management based on game-theoretic energy consumption scheduling for the future smart grid. *IEEE Trans. Smart Grid* **2010**, *1*, 320–331. [CrossRef]
54. Chao, H.; Hsieh, P.; Yang, T.; Hsiung, A. Model predictive optimization for distribution management in smart grids. In Proceedings of the IECON 2016-42nd Annual Conference of the IEEE Industrial Electronics Society, Florence, Italy, 23–26 October 2016; pp. 3984–3989.
55. Boyd, S.; Vandenberghe, L. *Convex Optimization*; Cambridge University Press: Cambridge, UK, 2004.
56. Deng, R.; Yang, Z.; Hou, F.; Chow, M.-Y.; Chen, J. Distributed Real–Time Demand Response in Multiseller–Multibuyer Smart Distribution Grid. *IEEE Trans. Power Syst.* **2015**, *30*, 2364–2374. [CrossRef]
57. Xu, D.; Zhong, F.; Bai, Z.; Wu, Z.; Yang, X.; Gao, M. Real-time multi-energy demand response for high-renewable buildings. *Energy Build.* **2023**, *281*, 112764. [CrossRef]
58. Trichakis, N.; Zymnis, A.; Boyd, S. Dynamic network utility maximization with delivery contracts. *IFAC Proc. Vol.* **2008**, *41*, 2907–2912. [CrossRef]
59. Duan, L.; Zhang, X.; Balta-Ozkan, N.; Etminan, S. Design and operation of solar-hydrogen-storage integrated electric vehicle charging station in smart city. In Proceedings of the CIRED 2021 Conference, Geneva, Switzerland, 20–23 September 2021. [CrossRef]
60. Barakat, S.; Samy, M.M. A Hybrid Photovoltaic/Wind Green Energy System for Outpatient Clinic Utilizing Fuel Cells and Different Batteries as a Storage Devices. In Proceedings of the 2022 23rd International Middle East Power Systems Conference (MEPCON), Cairo, Egypt, 13–15 December 2022; pp. 1–6.
61. Allan, M. Hydrogen Cars: How the Fuel Cell Works, Where the UK's Filling Stations Are and How Expensive They Are to Run. The Scotsman. Available online: https://www.scotsman.com/lifestyle/cars/hydrogen-cars-how-the-fuel-cell-works-where-the-uks-filling-stations-are-and-how-expensive-they-are-to-run-1386285# (accessed on 23 November 2023).